[redacted]

[redacted]

223

Copy

RM L52D21

NACA RM L52D21

TECH LIBRARY KAFB, NM

0144361

NACA

RESEARCH MEMORANDUM

7324

EFFECTS OF PLAN FORM, AIRFOIL SECTION, AND ANGLE OF ATTACK ON THE PRESSURES ALONG THE BASE OF BLUNT-TRAILING-EDGE WINGS AT MACH NUMBERS OF 1.41, 1.62, AND 1.96

By Kennith L. Goin

Langley Aeronautical Laboratory
Langley Field, Va.

CLASSIFIED DOCUMENT

[redacted]

NATIONAL ADVISORY COMMITTEE FOR AERONAUTICS

WASHINGTON

September 16, 1952

[redacted]

Classification cancelled (or changed to Unclassified)

By Authority of NASA Tech. Pub. Announcement 74 30 54
(OFFICER AUTHORIZED TO CHANGE)

By ..... NAME

GRADE OF OFFICER MAKING CHANGE)

10 Feb 62
DATE

TECH LIBRARY KAFB, NM

0144361

NATIONAL ADVISORY COMMITTEE FOR AERONAUTICS

RESEARCH MEMORANDUM

EFFECTS OF PLAN FORM, AIRFOIL SECTION, AND ANGLE OF ATTACK ON THE PRESSURES ALONG THE BASE OF BLUNT-TRAILING-EDGE WINGS AT MACH NUMBERS OF 1.41, 1.62, AND 1.96

By Kennith L. Goin

SUMMARY

An investigation has been made at Mach numbers of 1.41, 1.62, and 1.96 to determine the effects of airfoil section and wing plan form on the pressures acting along the base of blunt-trailing-edge wings operating through an angle-of-attack range. The investigation included two groups of untapered wings of aspect ratio 2.7, the first group being unswept and the second group having 45° of sweepback. Each group included airfoil sections with maximum thickness ratios of 3 to 10 percent and with varying amounts of trailing-edge bluntness. Also included in the investigation to indicate additional effects of wing plan form were a 45° delta wing and a rectangular wing of aspect ratio 5.0. All wings were tested with fixed transition at Reynolds numbers of between 1×10^6 and 2×10^6.

Spanwise variations of base pressures on rectangular wings were such that two-dimensional base pressures could probably be used with a fair degree of accuracy in estimating the base drag of such wings. For swept wings, however, the spanwise variations were very large.

Average base pressures decreased slightly with increases in angle of attack except in cases for which the boundary layers were believed to be separated or unusually thick. In such cases the base-pressure variations were generally characterized by rather abrupt increases followed by decreases as the angles of attack were increased.

The effects of changes in airfoil section on average base pressures were greater for the swept wing than for the unswept wing but were in all cases relatively small. The most important section parameter influencing average base pressures appeared to be the ratio of trailing-edge thickness to maximum thickness.

AFB 1764

Maximum variations in average base pressures resulted from variations in wing sweep and taper and in Mach number. The Mach number component normal to the wing leading edge appeared to be one of the more fundamental parameters influencing variations of base pressure coefficient at Mach numbers of 1.41 and 1.62. At a Mach number of 1.96, however, the Mach number component normal to the wing trailing edge appeared to be of greater importance.

Results obtained from previous base-pressure investigations by free-flight, wind-tunnel, transonic-bump, and wing-flow techniques have been summarized and compared with results of the present investigation. All results were found to be in good general agreement.

INTRODUCTION

Recent experimental investigations have shown that wings having blunt-trailing-edge sections will in some cases have higher lift-curve slopes, lower minimum drag, and higher maximum ratios of lift to drag at supersonic speeds than corresponding wings having sharp-trailing-edge sections (ref. 1). In consideration of these improved aerodynamic characteristics, together with obvious structural advantages, blunt-trailing-edge wings appear very promising for use at supersonic speeds.

Considerable experimental information on wing base pressures at Mach numbers of 1.5 to 3.1 is presented in reference 2. Although limited variations with spanwise location and angle of attack are included in reference 2, most of the base pressures were measured near the midsemispan position on rectangular wings of aspect ratio 3.0 and were obtained at 0° angle of attack. Limited data with similar restrictions for Mach numbers of 0.6 to 1.6 are included in references 3, 4, and 5. For estimations of wing base drag, considerably more information is needed concerning the variation of base pressures with spanwise location, with angle of attack, and with wing plan form.

As part of an investigation of wings with blunt-trailing-edge sections at Mach numbers of 1.41, 1.62, and 1.96, base pressures have been measured along the spans of 21 wings at angles of attack of 0° to 15°. Results of this base-pressure investigation are presented herein and include representative effects of wing plan form and detailed effects of wing section.

SYMBOLS

M	Mach number
R	Reynolds number
p_b	base pressure
p_s	free-stream static pressure
q	free-stream dynamic pressure
H	free-stream total pressure
P_b	base pressure coefficient, $\frac{p_b - p_s}{q}$
$P_{b'}$	average base pressure coefficient
P_{b_v}	pressure coefficient for zero base pressure, $-p_s/q$
α	angle of attack, degrees
A	aspect ratio
Λ	sweep of wing leading edge
λ	wing taper ratio, $\frac{\text{Tip chord}}{\text{Root chord}}$
b	wing span
c	wing chord
l	length of trailing-edge bevel
t	maximum wing thickness
h	wing thickness at trailing edge
s	spanwise distance from wing-fuselage juncture to wing tip
y	arbitrary spanwise distance, measured outboard from wing-fuselage juncture

x arbitrary distance along body axis, measured from nose of body

r local radius of body

DESCRIPTION OF MODELS

The geometric details of the 21 semispan wing models tested are given in figure 1(a) and the various wing sections are illustrated in figure 1(b). Each of the wings had symmetrical, straight-sided sections, polished surfaces, and a slightly rounded leading edge with a radius of approximately 0.002 inch. Each wing was equipped with four 0.030-inch-diameter pressure orifices located at the intersection of the wing-chord plane with the blunted trailing edge. The spanwise positions of the orifices measured outboard from the surface of the half-fuselage (half-body of revolution) were 20, 45, 65, and 83 percent of the exposed semispan for the delta wing and 20, 45, 70, and 95 percent of the exposed semispan for all other wings. Details of the half-fuselage used in all tests except those to determine effects of wing location and body size are shown in figure 2. A longer body, with the nose shape shown in figure 2, was used in tests to determine the effects of wing location. A body with a nose shape similar to that shown in figure 2, but having x and r coordinates increased by 50 percent, was used in tests to determine the effects of body size.

TUNNEL

The tests were conducted in the Langley 9- by 12-inch supersonic blowdown tunnel which utilizes the compressed air of the Langley 19-foot pressure tunnel. The compressed air is conditioned to insure condensation-free flow in the test section by being passed through a silica gel drier and through banks of finned electrical heaters. Turbulence damping screens are located in the tunnel settling chamber. The absolute stagnation pressure of the air entering the test section ranges from about 2 to $2\frac{1}{3}$ atmospheres. The three test-section Mach numbers are provided by use of interchangeable nozzle blocks.

Properties of the conditioned air and deviations of flow conditions in the test section with the tunnel clear, as determined from extensive

calibration tests and reported in reference 6, are presented in the following table:

Variable \ Nominal Mach number	1.41	1.62	1.96
Maximum dew-point temperature, °F	20	-5	-20
Minimum stagnation temperature, °F	120	125	165
Maximum deviation in Mach number	±0.02	±0.01	±0.02
Maximum deviation in ratio of static to stagnation pressure, p_s/H, percent	±2.0	±1.3	±2.2
Maximum deviation in stream angle, deg	±0.25	±0.20	±0.20

TEST TECHNIQUE

Details of the model test arrangement are shown in figure 2. Each semispan wing, and attached half-fuselage, was cantilevered from the tunnel wall. The half-fuselage was shimmed out 1/4 inch from the tunnel wall to minimize the effects of the tunnel-wall boundary layer on the flow over the fuselage (ref. 7). A clearance gap of 0.010 to 0.020 inch was maintained between the fuselage shim and the tunnel wall.

All the wings were tested with fixed transition for reasons discussed in appendix A. Transition was fixed by means of bands of roughness (carborundum grains having maximum dimensions of about 0.004 inch) cemented to the wings with thin films of shellac and extending over the complete exposed semispan of the upper and lower wing surfaces. The bands of roughness on the untapered wings were of about 5-percent-chord width and were located approximately between the 10- and 15-percent-chord location. This location was chosen after preliminary tests to determine the effects of boundary-layer momentum thickness on base pressures (appendix B) had indicated the effects of location of roughness to be, in general, relatively small. Bands of roughness on the delta wing were of constant $\frac{1}{8}$-inch width and consequently covered varying percentages of the wing chord. The ability of the bands of roughness to promote transition are clearly illustrated by flow studies of one of the swept wings, discussed in appendix B.

The Reynolds numbers varied during tests of each wing and also between tests of the different wings because of varying reservoir

stagnation pressures. The average Reynolds number based on mean aerodynamic chord for all the tests are shown in the following table:

Mach number	Average R (untapered wings)	Average R (delta wing)
1.41	1.6×10^6	1.8×10^6
1.62	1.4	1.7
1.96	1.3	1.5

Maximum deviations from these average values during the course of the investigation were about $\pm 0.2 \times 10^6$.

Pressures at the four spanwise orifices of the models and the tunnel stagnation pressure used in reducing the data were recorded simultaneously by photographing a multitube mercury manometer.

During the course of the investigation, a series of flow studies were made by use of a liquid-film technique. The technique, as discussed in reference 8, consists of spraying a thin film of liquid over the surface of a model having a black finish, testing the model until a flow pattern is established in the film, and then dusting the surface of the model with a light powder. Because of their greater shear intensities, turbulent boundary layers evaporate the film more rapidly than laminar boundary layers. When the model is dusted after testing, the powder adheres only to the wet portions of the surface (laminar-flow regions), and laminar-flow regions therefore appear light in photographs of the model while turbulent regions appear dark. There are exceptions to this which must be noted in the interpretation of liquid-film photographs: (1) When a laminar boundary layer is very thin, for instance near the wing leading edge, it has high shear intensities and consequently dries the film at rates equal to or greater than those for a turbulent boundary layer and (2) in regions of turbulent separation, and in regions where the turbulent boundary layer is very thick, the high shearing stresses of the turbulent boundary layer are not concentrated at the surface of the wing; consequently, the drying rate is slower than in regions where a turbulent boundary layer is relatively thin and attached to the surface or where a laminar boundary layer is very thin. As a matter of interest, the liquid used in the studies was a mixture of 15 parts alcohol, one part of glycerin, and a small amount of aerosol.

ACCURACY OF DATA

Ratios of static pressure to total pressure, obtained from tunnel-clear calibration tests, varied a maximum of 2.2 percent from average values in the vicinity of the test section occupied by the wings. Maximum corresponding Mach number variations were ±0.02. It would appear that the effects on base pressures of such nonuniform flow conditions would result not so much from the actual flow variations as from the intersection with the model boundary layer of the characteristic disturbances which cause the variations. Such disturbances might be expected to affect base pressures by causing transition or separation of the boundary layer. During the present tests, however, transition was fixed on the wings. Because turbulent boundary layers are inherently stable, a weak disturbance would not be expected to cause separation and consequently it is believed that the base pressures presented herein are not appreciably influenced by varying tunnel flow conditions.

Although it is believed that actual base pressures are not influenced to an appreciable extent by the varying flow conditions in the test section, the calculated pressure coefficients $\left(\frac{p_b - p_s}{q}\right)$ can vary over a considerable range, depending on the value of p_s/H used in determining the reference static pressures. For instance, the differences between coefficients calculated using the mean and the extreme tunnel-clear calibration values of p_s/H to determine reference static pressures would be about ±0.060 at a Mach number of 1.96. In order to reduce the data to coefficient form, it was necessary to assume fixed values of p_s/H for each Mach number and then to calculate the reference static pressures using measured values of H. Mean values of p_s/H, obtained from tunnel-clear calibration tests, were used in these calculations and, because they are logically more representative than the extreme values, it is believed that inaccuracies in $\frac{p_b - p_s}{q}$, resulting from the use of improper values of p_s/H, are only a small percentage of the value mentioned above.

The nominal angle-of-attack settings of the models with respect to the tunnel center line were 0°, $\pm 3^\circ$, $\pm 6^\circ$, $\pm 9^\circ$, $\pm 12^\circ$, and $\pm 15^\circ$. The actual angles, within $\pm 0.05^\circ$, are as follows:

α, deg	α, deg
-15.29	14.94
-12.17	11.93
-9.08	8.95
-6.03	5.99
-3.00	3.00
	0

Because the models were symmetrical and the variations of base pressures with angle of attack were in general very small, the pressure coefficients at negative and positive angles of attack were averaged and the results are presented using the following average absolute values of angle of attack:

α, deg	Accuracy, deg
15.11	±0.23
12.05	±.17
9.01	±.12
6.01	±.07
3.00	±.05
0	±.05

The assumption that the base pressures for the slightly different negative and positive angles of attack were for practical purposes equal allowed a more straightforward and compact presentation of the data with no significant loss in accuracy.

The pressures at the two angles of attack were used to determine the repeatability of the data. In comparing 1576 pressure coefficients at positive angles of attack with corresponding pressure coefficients at negative angles of attack, it was found that the coefficients checked within ±0.005 in 84 percent of the cases, within ±0.010 in 97 percent of the cases, and within ±0.015 in 99.2 percent of the cases. The possible inaccuracies of the calculated pressure coefficients due to inaccuracies of reading the heights of mercury columns from film records was estimated to be about ±0.005.

RESULTS AND DISCUSSION

Effects of wing location and body size.- A preliminary investigation was made to determine the effects on base pressures of wing location on

the fuselage and also of fuselage size. The wings used in the investigation had 0° and 45° of leading-edge sweep and 6-percent-thick sections with fully blunted trailing edges. Results are presented in figure 3 where average base pressure coefficients, obtained numerically by application of Simpson's rule, are plotted as functions of angle of attack. Figures 3(a) and 3(b) illustrate the effects of varying the locations of the swept and unswept wings on the fuselage described in figure 2. Figure 3(c) shows the base pressure coefficients for the unswept wing located at two positions on a body having x and r ordinates increased 50 percent over those of the body shown in figure 2. Base pressure coefficients for the wing on the smaller body are also presented in figure 3(c) for purposes of comparison.

The data of figures 3(a) and 3(b) indicate decreasing base pressures as the wings are moved forward on the body up to a limiting location, after which further movement causes no appreciable effect on base pressure. These results are believed to be due to the fact that, as the wing is moved forward, the wing trailing edge is further displaced from the intersection with the wing wake of the wall-reflected disturbance originating at the nose of the body. Since no appreciable effects of wing location are shown when the wing is located far enough forward, it would appear that the flow over the body does not appreciably influence base pressures. This would appear especially true since the flow changes much more rapidly over the forward portion of a body than over the rearward portion. Figure 3(c) shows that in the forward positions the base pressures for the rectangular wing on the large and small body are essentially the same; these results also indicate no appreciable effect of flow over the body on base pressures.

All subsequent base-pressure measurements were obtained with the wings located far enough forward on the small fuselage to avoid the effects of location shown in figure 3. The distances from the fuselage nose to the wing leading edges were in most cases 6.0 fuselage radii for the swept wing and 7.0 fuselage radii for the unswept wing but were somewhat greater in a few cases at Mach numbers of 1.62 and 1.96.

Spanwise variations of base pressures.- The spanwise variations of base pressure coefficients for each of the models are presented in figure 4 at representative angles of attack of 0°, 6.01°, and 12.05°. Results for the rectangular wings of aspect ratio 2.7 are presented in figures 4(a) to 4(d). Results for the 45° swept untapered wings of aspect ratio 2.7 are presented in figures 4(e) to 4(h), and figures 4(i) and 4(j) present results for the rectangular wing of aspect ratio 5.0 and the 45° delta wing, respectively.

The data of figures 4(a) to 4(d) for the unswept wings show that at a Mach number of 1.41, and to a lesser extent at a Mach number of 1.62, the base pressure coefficients over the inner portion of the wings

having beveled trailing edges are much higher at 12.05° than at 0° and 6.01° angle of attack. The probable reason for these higher pressures is indicated by the liquid-film photographs of figure 5 which show light regions (regions in which the boundary layer did not dry the liquid film) over the inner portion of the upper surface of a beveled-trailing-edge wing at 13° and 14° angle of attack. The light regions indicate the presence of separated boundary layers or of unusually thick attached boundary layers, either of which might be expected to result in higher base pressures by decreasing the amount of expansion around the corner at the wing trailing edge. In order to try to establish the presence or absence of flow separation, additional studies were made in which a liquid was bled through two orifices in the trailing edge of the wing shown in figure 5. At a Mach number of 1.41 and angles of attack of 13° and 14°, the liquid flowed up on to the upper surface of the wing and forward but did not completely cover the light regions of the wing shown by the photographs of figure 5. The fact that the liquid flowed forward proves that some separation existed but it does not establish the fact that the light regions are indications only of separation.

The data of figures 4(a) to 4(d) show that spanwise variations in base pressures for the rectangular wings are in general not large except at high angles of attack on wings having beveled or relatively thin trailing edges. They show that the magnitude of the spanwise variations, as well as the changes in pressure distribution due to angle of attack and due to wing section, decreases with increasing Mach number. The fact that the spanwise pressure variations are not large appears to indicate that two-dimensional base pressures could be used with a fair degree of accuracy in estimating the base drag of three-dimensional rectangular wings.

The data of figures 4(e) to 4(h) show very large spanwise variations in base pressure for the untapered 45° swept wings at Mach numbers of 1.41 and 1.62. These large variations may be due in part to spanwise flow along the base of the wings and to tip effects which are different from those for the rectangular wings. They are apparently not due to flow separation or unusually thick boundary layers because large variations are shown in the last plot of figure 4(e) at a Mach number of 1.41 and 0° angle of attack, whereas the liquid-film photograph for the same wing at 0° angle of attack (fig. 6) gives no indication of such conditions except near the wing-fuselage juncture. As was the case for unswept wings, the spanwise variations become smaller as the Mach number is increased.

The data of figure 4(i) show only moderate spanwise base-pressure variations for the rectangular wing of aspect ratio 5.0. Somewhat larger variations are shown in figure 4(j) for the 45° delta wing, but the spanwise pressure variations for this wing are much more regular than those

for the 45° swept untapered wings. It might be pointed out that the high-aspect-ratio and the 45° delta wings were large enough to cause tunnel blocking at the higher angles of attack and lower Mach numbers, and data for these conditions in figures 4(i) and 4(j) are therefore not included.

Variations of average base pressure coefficients with angle of attack.- The average base pressure coefficients for all the unswept wings are presented in figure 7 as functions of wing angle of attack; those for the 45° swept wings are presented in figure 8. It should be mentioned that the average pressure coefficients for all the untapered wings were obtained by assuming the spanwise distributions shown by the faired curves of figures 4(a) to 4(i), and similar curves for angles of attack not shown in figure 4, and numerically integrating along the span. In the case of the 45° delta wing, average base pressures were obtained by weighting the pressures according to trailing-edge thickness and then performing similar integrations.

In general, the data of figure 7 show small decreases in the average base pressures for rectangular wings as the angle of attack is increased to 6° or more. At angles of attack above 6° the base pressures for the wings having the greater amount of trailing-edge bevel increase very rapidly with further increases in angle of attack, particularly at a Mach number of 1.41. As previously discussed these increases are probably due either to flow separation or to increased thickness of the boundary layer. The data show that for the wing having the greatest amount of trailing-edge bevel $\left(\frac{t}{c} = 0.10;\ \frac{h}{t} = 0.375;\ \frac{l}{c} = 0.20\right)$ a lower limit of average base pressure is reached after which further increases in angle of attack cause slight decreases in base pressure.

The data of figure 8 for the 45° swept wings show that, as the angle of attack is increased from zero, average base pressures decrease for wings having full blunt sections, whereas increases are shown for wings having beveled trailing edges. The increasing pressures for the beveled-trailing-edge wings reach maximum values at angles of attack which appear to depend on the amount of bevel, after which further increases in angle of attack result in lower pressures. These trends are somewhat similar to those for the rectangular wings. The principal difference appears to be that the effect of beveling the trailing edge of the swept wings is more pronounced and occurs at lower angles of attack than for the rectangular wings. This might be due in part to the larger angles of bevel and the lower Reynolds number of the swept wings in planes normal to the wing leading edge.

Variations of average base pressure coefficients with wing section.- The ratios of average base pressure coefficient to the pressure coefficient

for a vacuum P_b'/P_{b_v} are presented in figures 9 and 10 as functions of the ratio of trailing-edge thickness to maximum thickness h/t. The ordinate P_b'/P_{b_v} was used in these summary figures because it has been found to be an important base-pressure parameter in analyses for determining optimum wing sections.

Only moderate variations in base pressure with wing section are shown in figure 9 for the unswept wings and it can be seen that the base pressures correlate very nicely at angles of attack of 0°, 3.00°, and 6.01° when plotted against h/t. At the higher angles of attack, however, pressures for some of the wings deviate from the trends indicated at lower angles of attack. These deviations are indicated by dashed lines in the plots for 9.01°, 12.05°, and 15.11° angle of attack and, as previously memtioned, are probably a result of flow separation or unusually thick boundary layers.

The data of figure 10 show that the base pressures for the 45° swept wings also correlate nicely when plotted as functions of h/t. Deviations believed due to separation or unusually thick boundary layers occur at angles of attack considerably lower than those for the unswept wings, however, possibly because of the lower Reynolds numbers in planes normal to the wing leading edge and also because of the greater amounts of trailing-edge bevel in the same plane. The plots for 9.01°, 12.05°, and 15.11° show that, after the base pressures begin to deviate from average curves, the pressures for each value of maximum thickness ratio correlate very well when plotted against h/t but that the importance of maximum thickness ratio t/c becomes of the same order as the ratio h/t.

Effects of plan form.- The summary variations with wing section of the data for the 0° and 45° swept wings at angles of attack of 0°, 3°, and 6.01° from figures 9 and 10 are compared in figure 11 (data for which the boundary layer was believed to be separated or unusually thick are omitted). The data of figure 11 show that the base pressures for the swept wings are lower than those for the unswept wings at Mach numbers of 1.41 and 1.96 but are about equal to those for the unswept wings at a Mach number of 1.62. They show that the effects of thickening the trailing edge are opposite for the swept and unswept wings at Mach numbers of 1.41 and 1.62 but are the same at a Mach number of 1.96. It seems possible that some of these seeming irregularities may be a result of transonic flow characteristics in the case of the 45° swept wings. In order to obtain some idea as to whether this is true, data from figure 11, together with data for the 45° delta wing and the aspect ratio 5.0 wing have been plotted as functions of the Mach number component normal to wing leading edge in figure 12. The representative data of figure 12 show that base pressure for all the wings, with the exception of the 45° delta wing at $M = 1.96$, correlate fairly well when plotted as

functions of $M \cos \Lambda$. This generally good correlation tends to indicate the Mach number component normal to the wing leading edge to be one of the more fundamental parameters influencing base pressures. The fact that the base pressures for the delta wing at $M = 1.96$ are nearer to those for the rectangular wing of similar section than to those for the 45° swept untapered wing would, however, appear to indicate the Mach number component normal to the trailing edge to be of greater importance at $M = 1.96$. These indications that effects of plan form vary with Mach number make the use of $M \cos \Lambda$ for correlation appear somewhat idealistic. Tests of additional tapered wings would be needed to explain these results.

Comparison with data from other facilities.- In figure 13, a general comparison is made between the zero angle-of-attack data of figure 12 and data presented in references 2, 3, 4, and 5. Data from references 2 to 5 were obtained from tests in the Ames 1- by 3-foot supersonic tunnels at Mach numbers of 1.5, 2.0, and 3.1, by free-flight rocket tests at Mach numbers of 0.6 to 1.6, by the NACA wing-flow method at Mach number of 0.7 to 1.2, and by the bump test technique in the Ames 16-foot high-speed tunnel at Mach numbers of 0.6 to 1.1.

The data from reference 2 are local base pressures measured at near the midsemispan location on a series of rectangular wings of aspect ratio 3.0 with fixed transition. Maximum wing thickness ratios were 5, $7\frac{1}{2}$, and 10 percent and values of h/t were 1/4, 1/2, 3/4, and 1.0. The data from reference 2 included in figure 13 have been restricted to those for which the ratios of boundary-layer thickness to trailing-edge thickness are relatively small $\left(\frac{c}{hR^{1/5}}\right.$ between 0.5 and 2.25, which is the approximate range of the present investigation$\left.\right)$ because these cases are representative of the higher Reynolds numbers. It should be mentioned that at Mach numbers of 1.5 and 2.0 the width of the band in which the data of reference 2 lie (fig. 13) results almost entirely from random scatter. At a Mach number of 3.1, however, there is very little random scatter and the width of the band is determined almost entirely by the variation of $\frac{c}{hR^{1/5}}$. The higher values of P_b/P_{b_v} shown at a Mach number of 3.1 were obtained at the lower values of $\frac{c}{hR^{1/5}}$.

The data from reference 3 were obtained from free-flight tests of a rectangular wing of aspect ratio 2.7 at Reynolds number of 5×10^6 to 9×10^6. The wing had a 6-percent-thick full blunted section, similar

to one of wings of the present investigation. Base pressures were obtained by means of two slots located in the trailing edge of the wing and extending from 38 to 62 and from 52 to 76 percent of the exposed wing semispan.

The data of reference 4 were obtained from tests by the bump technique of rectangular wings having aspect ratios of 4.0 and modified 4-percent-thick circular-arc sections with ratios of trailing-edge thickness to maximum thickness of 0.3, 0.6, and 1.0. Pressures were measured by means of orifices located at 25.0-, 37.5-, 62.5-, and 87.5-percent-semispan stations and the data presented in figure 13 are averages of the pressures over the portions of the wing trailing edge between the 25.0- and 87.5-percent-semispan stations.

The data of reference 5 were obtained from tests by the NACA wing-flow method of a rectangular wing of aspect ratio 8 with 14-percent-thick wedge airfoil sections. Orifices located in the base of the wing at 5.0-, 12.5-, 40.0-, and 80.0-percent-semispan stations were used for the pressure measurements. Pressures measured at the outer orifice lie along the lower boundary of the band shown in figure 13, whereas those measured at the inner three orifices are concentrated near the upper boundary of the band.

It should be pointed out that the data of references 4 and 5 were obtained without fixed transition at relatively low Reynolds numbers (1.7×10^6 to 2.2×10^6 in ref. 4 and 0.4×10^6 to 0.7×10^6 in ref. 5) and that the wing boundary layers were therefore possibly laminar. The validity of a comparison of these possibly laminar-flow data with those for turbulent flow is questionable in consideration of the important effects of boundary layer shown in reference 2. These data constitute most of the known data in the transonic Mach number range, however, and are therefore believed to be of sufficient interest to include in the general comparisons in figure 13.

Figure 13 shows very good agreement between the local base pressures of references 2 and 3 with average base pressures for the rectangular wings of the present investigation. At the lower values of $M \cos \Lambda$, where the data of the present investigation were obtained from tests of 45° swept wings, however, there are sizable discrepancies between data from reference 3 and average base pressures from the present investigation The greater part of these discrepancies can probably be attributed to effects of sweep which, from figure 12, appear to be secondary to effects of the normal Mach number component except in the case of the 45° delta wing at a Mach number of 1.96. Some of the discrepancies can also be attributed to the fact that base pressures from reference 3 were measured from slots located near the wing midsemispan and are therefore not

necessarily indicative of average base pressures because of spanwise variations such as those shown in figure 4.

It is interesting to note that the agreement of the data of references 4 and 5 with average base pressures from the present investigation is about as good as that shown for the data of reference 3.

Figure 13 shows that data from the various facilities are in general agreement in spite of the widely varied conditions under which they were obtained. It is believed that these data will be useful for many general engineering applications even though variations of the order of ±20 percent are shown in some cases at given values of $M \cos \Lambda$ greater than 1.0. For instance, on a wing with a half-blunt trailing edge it would be expected that the base drag would be of the order of one-fourth the total pressure drag at supersonic speeds. If the wing were relatively thin, friction drag could easily amount to one-half the total wing drag, in which case the base drag would be only one-eighth of the total wing drag. Variations of ±20 percent in base pressures would in such a case amount to only $2\frac{1}{2}$-percent variations in total wing drag and would therefore not be of serious consequence. The data should also be of value for use in conjunction with theories, such as those presented in references 9 and 10, from which optimum airfoils may be determined for various design criteria.

CONCLUDING REMARKS

An investigation of 21 wings with fixed transition has indicated the following results regarding base pressures at Mach numbers of 1.41, 1.62, and 1.96.

For blunted wings mounted on bodies of revolution, base pressures were not appreciably affected by body size or wing location.

The spanwise variations of base pressures on rectangular wings were such that two-dimensional base pressures could in general be used with a fair degree of accuracy in estimating the base drag of such wings. For swept wings, however, the spanwise variations of base pressure were very large.

Average base pressures decreased slightly with increases in angle of attack except in cases for which the boundary layers were believed to be separated or unusually thick. In such cases the base-pressure variations were generally characterized by rather abrupt increases followed by decreases as the angles of attack were increased.

The effects of changes in airfoil section on average base pressures were greater for the swept wing than for the unswept wing but were in all cases relatively small. The most important section parameter influencing base pressures appeared to be the ratio of trailing-edge thickness to maximum thickness.

Maximum variations in average base pressures resulted from changes in wing sweep and taper and in Mach number. The Mach number component normal to the wing leading edge appeared to be one of the more fundamental parameters affecting base pressure coefficients at the lower Mach numbers (1.41 and 1.62). At a Mach number of 1.96, however, the Mach number component normal to the trailing edge appeared to be more important.

Results obtained from previous base-pressure investigations by free-flight, wind-tunnel, transonic-bump, and wing-flow techniques have been summarized and compared with results of the present investigation. All results were found to be in general agreement.

Langley Aeronautical Laboratory
National Advisory Committee for Aeronautics
Langley Field, Va.

APPENDIX A

REASONS FOR TESTING WINGS WITH FIXED TRANSITION

Previous base-pressure measurements have indicated that considerable differences exist between the characteristics of base pressures with laminar and with turbulent flow in the boundary layer and that base pressures for the two types of flow must therefore be considered separately.

The present investigation has been limited to a study of base pressures on wings having fixed transition for the following reasons: (1) Turbulent-boundary-layer data should have a greater range of practical application than data for which the boundary layer is laminar because high flight Reynolds numbers and surface roughness due to manufacturing tolerances would tend to promote transition on flight configurations. (2) The boundary layers on the models without fixed transition were in most cases laminar over the greater part of the wing but were turbulent near the wing tip, as shown in Appendix B. Base pressures for the wings without fixed transition would therefore not be representative of either type of boundary layer. (3) Data presented in reference 2 indicate that base pressures for laminar flow are influenced to a large extent by Reynolds number, over which little control is possible in the present test facility, and that base pressures for turbulent flow are relatively independent of Reynolds number at Mach numbers of the present investigation.

Reference 2 presents wing base-pressure data obtained at low Reynolds numbers (below 2×10^6) during tests at a Mach number of 2.0 in which various width bands of lampblack grains, a strip of salt crystals and a wire strip were used to promote transition. Data are also presented for the smooth wing at Reynolds number above 2×10^6 with natural transition. No sizable differences are shown between the base pressures obtained at Reynolds numbers of 1×10^6 to 2×10^6 with the various artificial transition devices and those obtained at higher Reynolds numbers with natural transition. This would appear to indicate that at the Reynolds numbers of the present investigation (1.1×10^6 to 1.9×10^6) satisfactory base-pressure measurements with turbulent-boundary-layer flow can be obtained with artificial transition and that the type of artificial transition device used is not of primary importance.

APPENDIX B

RESULTS OF TESTS TO DETERMINE THE EFFECTS OF BOUNDARY-LAYER MOMENTUM THICKNESS ON BASE PRESSURES

In an effort to determine the effects on base pressures of boundary-layer momentum thickness, a series of tests were made in which transition was fixed at various chordwise positions on representative untapered wings of aspect ratio 2.7 and of 0° and 45° sweepback. The wing sections were 10-percent-thick and had ratios of trailing-edge thickness to maximum thickness h/t of 0.375. Base pressures were measured on the smooth wings and then on the wings with 5-percent-chord transition strips added to the upper and lower surfaces at various positions along the chords. Results of the tests are presented in figure 14 where the average base pressure coefficients are plotted as functions of angle of attack.

The data of figure 14 show that, at $M = 1.41$, the average pressure coefficients at low angles of attack increase as the transition strip is moved rearward. The effects of transition-strip location decrease with increase in angle of attack, however, and are insignificant at angles of attack greater than 9° for the unswept wing and greater than 6° for the swept wing. At Mach numbers of 1.62 and 1.96, no appreciable effects of transition-strip location are shown at any angle of attack. Since changes in momentum thickness are directly related to changes in the location of transition, these data appear to indicate the effects of changes in momentum thickness to be insignificant except at low angles of attack at $M = 1.41$, in which cases the effects appear significant but relatively small.

Aside from the effects of location of transition, there are some other interesting results shown in figure 14. At all Mach numbers, the base pressure coefficients for the smooth unswept wing are higher than those for the rough (transition fixed) wing at low angles of attack but are about equal to those for the rough wing at higher angles of attack. For the swept wings the effects of fixing transition are opposite to those for the unswept wing at $M = 1.41$ (base pressure coefficients for the smooth wing are lower) but are less pronounced. At Mach numbers of 1.62 and 1.96 the effects on swept-wing base pressures of fixing transition are very small.

Unswept wing.- The liquid-film photographs of figure 15(a) indicate that at a Mach number of 1.41, the flow over the smooth wing is mostly laminar up to angles of attack somewhat greater than 9°. In consideration of data presented in reference 2, higher base pressures for the smooth

wing than for the wing with transition fixed might therefore be expected up to fairly high angles of attack. The reason for the abrupt increase in base pressures for the rough wing at angles of attack between 9° and 12°, resulting in equal base pressures for the rough and smooth wing, is indicated by figure 5, as previously discussed, to be probably due either to flow separation or to thickening of the boundary layer.

The liquid-film photographs of figure 15(b) show that at a Mach number of 1.96, the regions of turbulent flow near the wing tip increase on both the upper and the lower surface as the angle of attack is increased (this is in contrast with an increase on the upper surface and a decrease on the lower surface at a Mach number of 1.41). These increasing regions of turbulent flow are probably responsible for the smooth-wing base pressures approaching those for the rough wing as the angle of attack is increased at Mach numbers of 1.62 and 1.96.

Swept wing.- The liquid-film photograph for the swept wing at a Mach number of 1.41 and 0° angle of attack (fig. 16(a)), indicates the boundary layer to be laminar except in a region near the trailing edge at the wing tip where turbulence is indicated (marked T). In addition to this region of turbulenece near the wing tip, there is one particularly dark area near the wing trailing edge (marked TL) which might at first appear to indicate turbulence. It will be noted, however, that the dark area originates at the wing-fuselage juncture and is followed by a light area which indicates a laminar boundary layer. Since it is highly improbable that a laminar flow would occur immediately downstream from a turbulent flow, it is believed that the dark area indicates a region of thin laminar boundary layer resulting from the expansion over the surface of the wing. From a comparison of this photograph with the similar photograph of the wing with roughness added (fig. 6), it can be seen that transition was fixed by the strip of roughness.

The fact that the base pressure for the rough wing is higher than that for the smooth wing at a Mach number of 1.41 and 0° angle of attack (fig. 14), is somewhat surprising in view of the opposite effect of fixing transition on the unswept wing. The higher base pressures for the rough wing at 6° angle of attack do not appear unreasonable, however, because figure 6 indicates either turbulent separation or thickening of the boundary layer over a large portion of the upper surface of the rough wing while none is shown for the smooth wing in figure 16. At 9° angle of attack, a flow pattern which appears to indicate turbulent separation or a thickened turbulent boundary layer is shown on the upper surface of the smooth wing. Considering the liquid-film photographs of figure 6, similar conditions would be predicted for the rough wing. Equal base pressures for the smooth and rough wing, as shown in figure 14, do not therefore appear unreasonable.

At a Mach number of 1.96, the boundary layers on both surfaces of the smooth wing at 0°, 6°, and 9° angles of attack are shown in figure 16(b) to be, for the most part, turbulent at the wing trailing edge. This type of flow would tend to explain the very nearly equal base pressures shown in figure 14 for the smooth and rough wings at Mach numbers of 1.62 and 1.96.

REFERENCES

1. Chapman, Dean R.: Reduction of the Profile Drag at Supersonic Velocities by the Use of Airfoil Sections Having a Blunted Trailing Edge. NACA RM A9H11, 1949.

2. Chapman, Dean R., Wimbrow, William R., and Kester, Robert H.: Experimental Investigation of Base Pressure on Blunt-Trailing-Edge Wings at Supersonic Velocities. NACA TN 2611, 1952.

3. Morrow, John D., and Katz, Ellis: Flight Investigation at Mach Numbers from 0.6 to 1.7 to Determine Drag and Base Pressures on a Blunt-Trailing-Edge Airfoil and Drag of Diamond and Circular-Arc Airfoils at Zero Lift. NACA RM L50E19a, 1950.

4. Cleary, Joseph W., and Stevens, George L.: The Effects at Transonic Speeds of Thickening the Trailing-Edge of a Wing with 4-Percent-Thick Circular-Arc Airfoil. NACA RM A51J11, 1951.

5. Sawyer, Richard H., and Daum, Fred L.: Measurements through the Speed of Sound of Static Pressures on the Rear of Unswept and Sweptback Circular Cylinders and on the Rear and Sides of a Wedge by the NACA Wing-Flow Method. NACA RM L8B13, 1948.

6. May, Ellery B., Jr.: Investigation of the Effects of Leading-Edge Chord-Extensions on the Aerodynamic and Control Characteristics of Two Sweptback Wings at Mach Numbers of 1.41, 1.62, and 1.96. NACA RM L50L06a, 1951.

7. Conner, D. William: Aerodynamic Characteristics of Two All-Movable Wings Tested in the Presence of a Fuselage at a Mach Number of 1.9. NACA RM L8H04, 1948.

8. Love, Eugene S.: Investigations at Supersonic Speeds of 22 Triangular Wings Representing Two Airfoil Sections for Each of 11 Apex Angles. NACA RM L9D07, 1949.

9. Chapman, Dean R.: Airfoil Profiles for Minimum Pressure Drag at Supersonic Velocities - General Analysis with Application to Linearized Supersonic Flow. NACA TN 2264, 1951.

10. Klunker, E. B., and Harder, Keith C.: Comparison of Supersonic Minimum-Drag Airfoils Determined by Linear and Nonlinear Theory. NACA TN 2623, 1952.

CONFIDENTIAL

Plan form				Section		
	A	λ	Λ	t/c	h/t	l/c
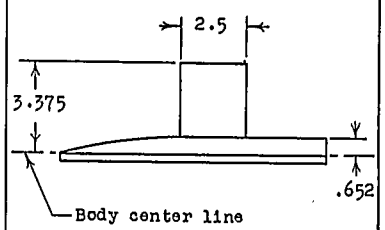	2.7	1.0	0°	0.100 .060 .045 .030	1.000 .500 .375 .375 .375 1.000 .500 1.000 .667 1.000	0 .20 .20 .35 .50 0 .20 0 .20 0
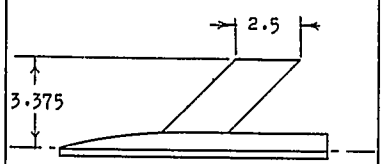	2.7	1.0	45°	.100 .060 .045 .030	1.000 .500 .375 .375 1.000 .500 1.000 .667 1.000	0 .20 .20 .35 0 .20 0 .20 0
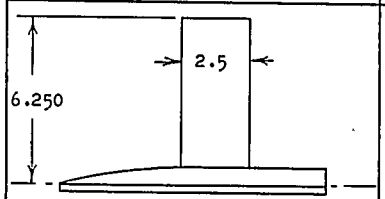	5.0	1.0	0°	.060	1.000	0
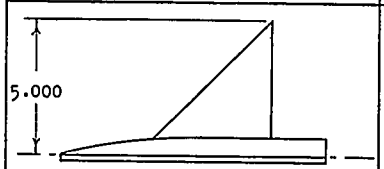	4.0	0	45°	.060	1.000	0

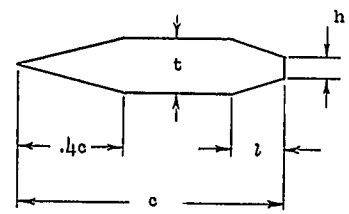

Streamwise Section

(a) Geometric details of models. (All dimensions in inches.)

Figure 1.- Plan form and section characteristics of wing models tested.

CONFIDENTIAL

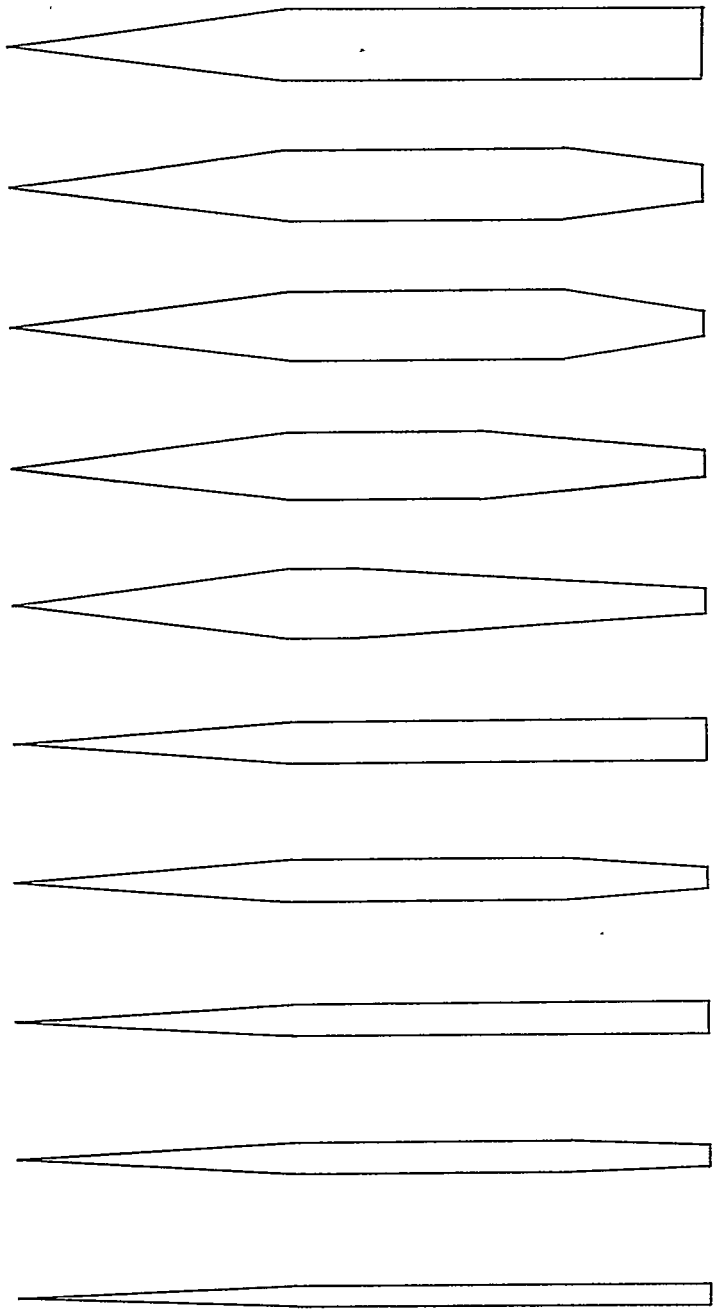

t/c	h/t	l/c
0.100	1.000	0
.100	.500	.20
.100	.375	.20
.100	.375	.35
.100	.375	.50
.060	1.000	0
.060	.500	.20
.045	1.000	0
.045	.667	.20
.030	1.000	0

(b) Illustration of various wing sections.

Figure 1.- Concluded.

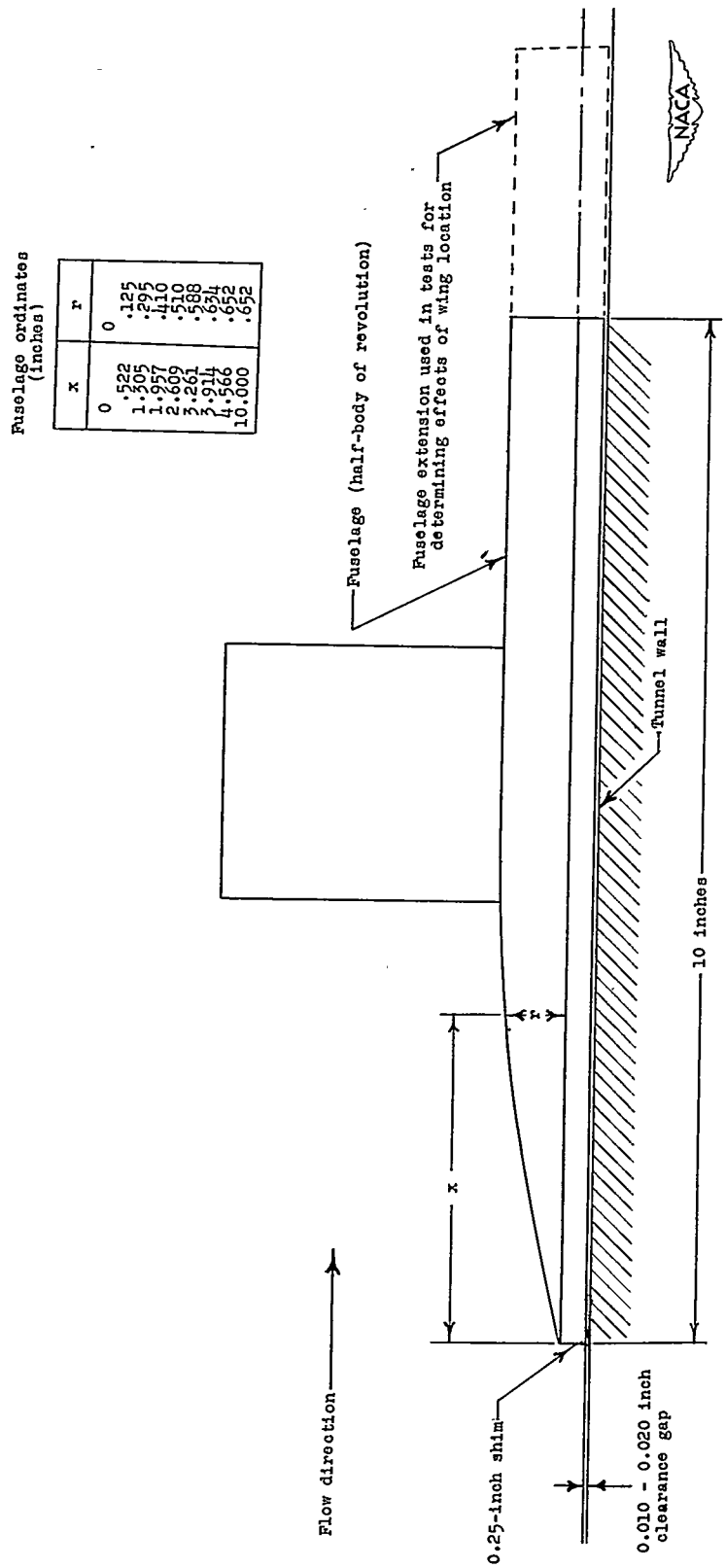

Figure 2.- Details of model mounting arrangement.

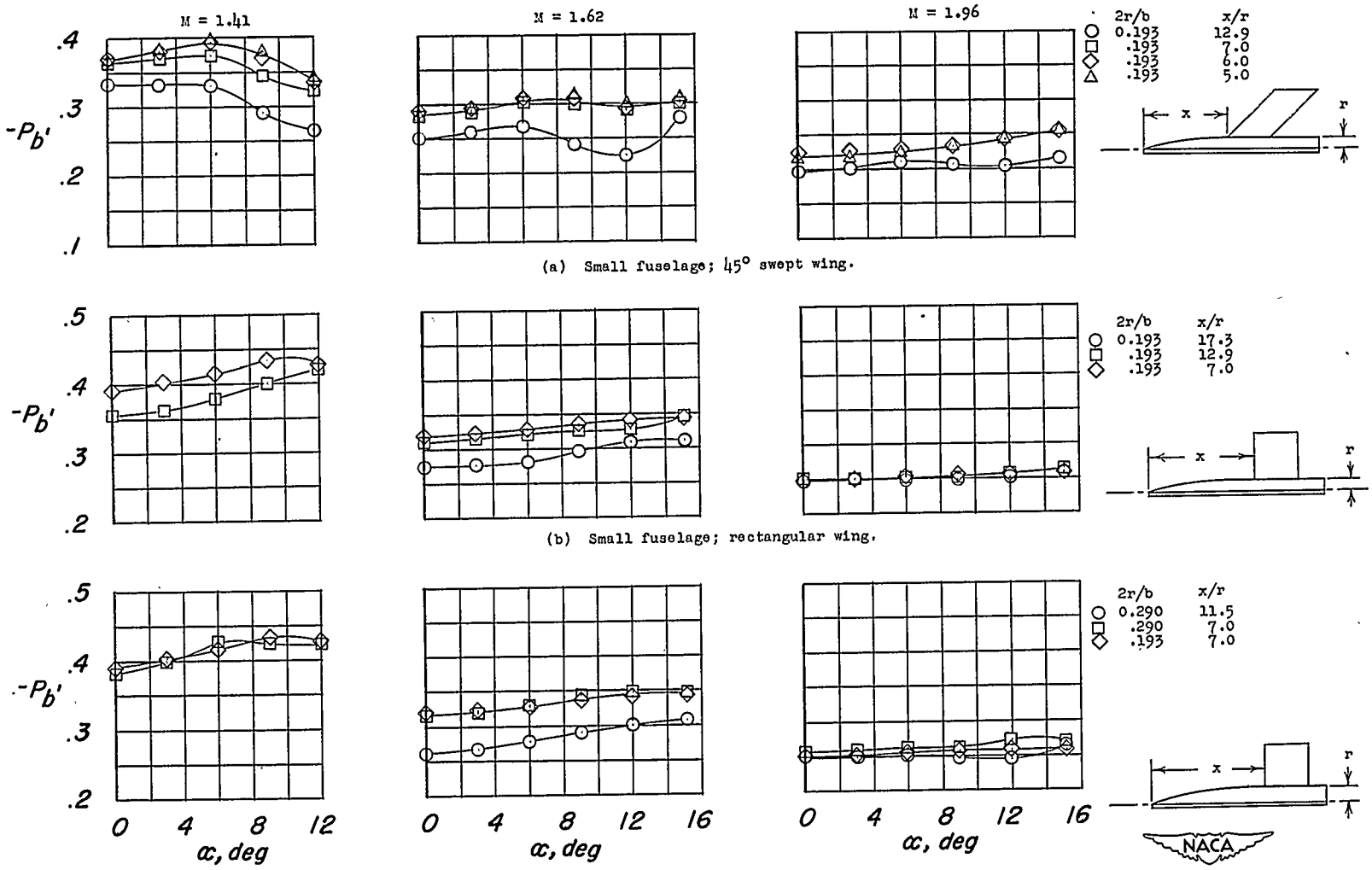

(a) Small fuselage; 45° swept wing.

(b) Small fuselage; rectangular wing.

(c) Large and small fuselages; rectangular wing.

Figure 3.- Effects of wing location and body size on average base pressure coefficients. $A = 2.7$; $\Lambda = 0^\circ$ and 45°; $\lambda = 1.0$; $\frac{t}{c} = 0.060$; $\frac{h}{t} = 1.000$.

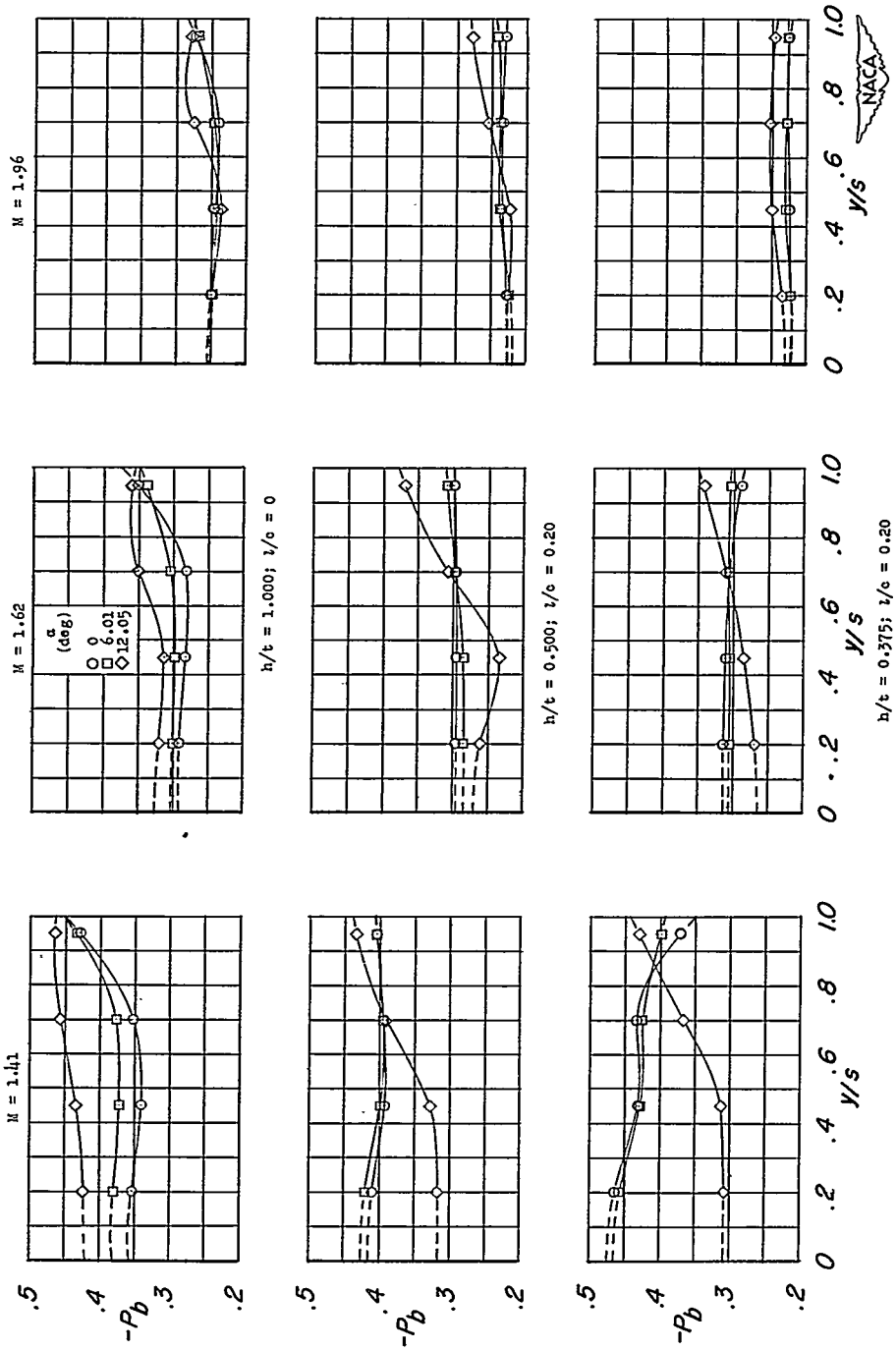

Figure 4.- Representative spanwise distributions of base pressure.

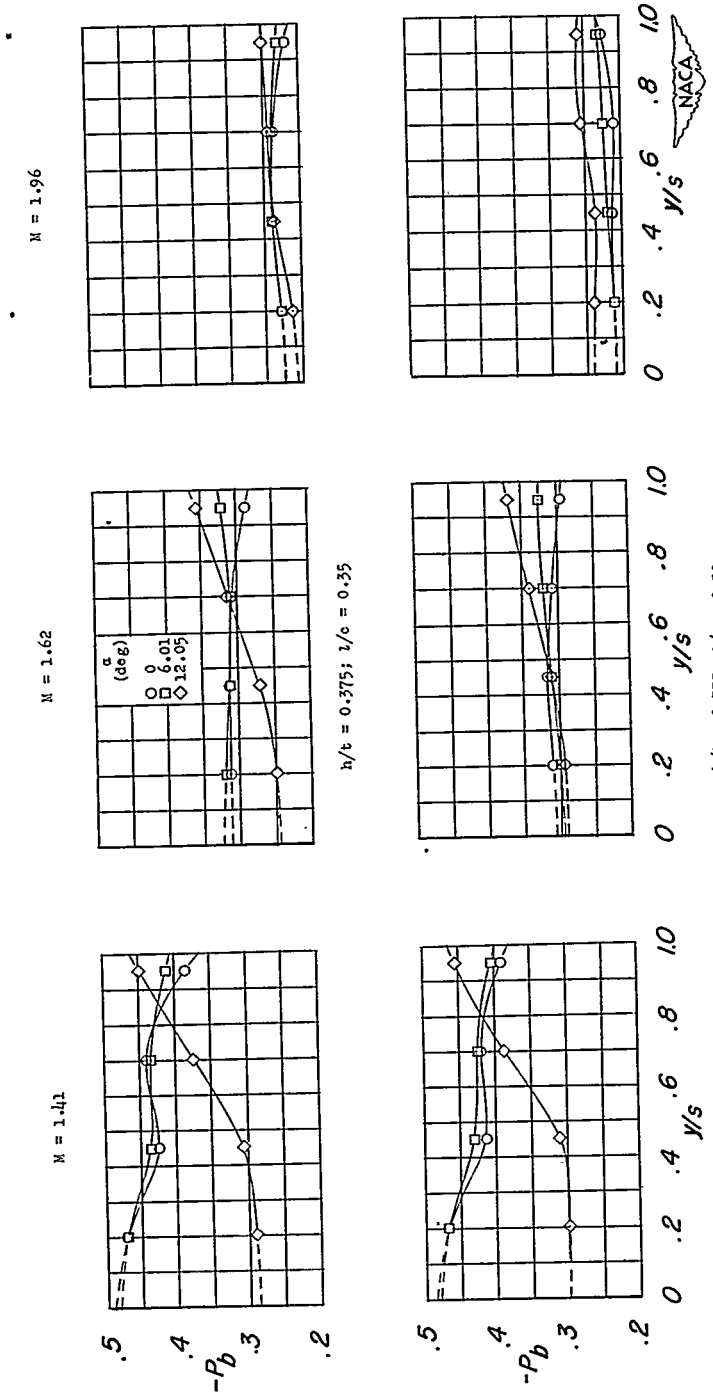

(a) Concluded.

Figure 4.- Continued.

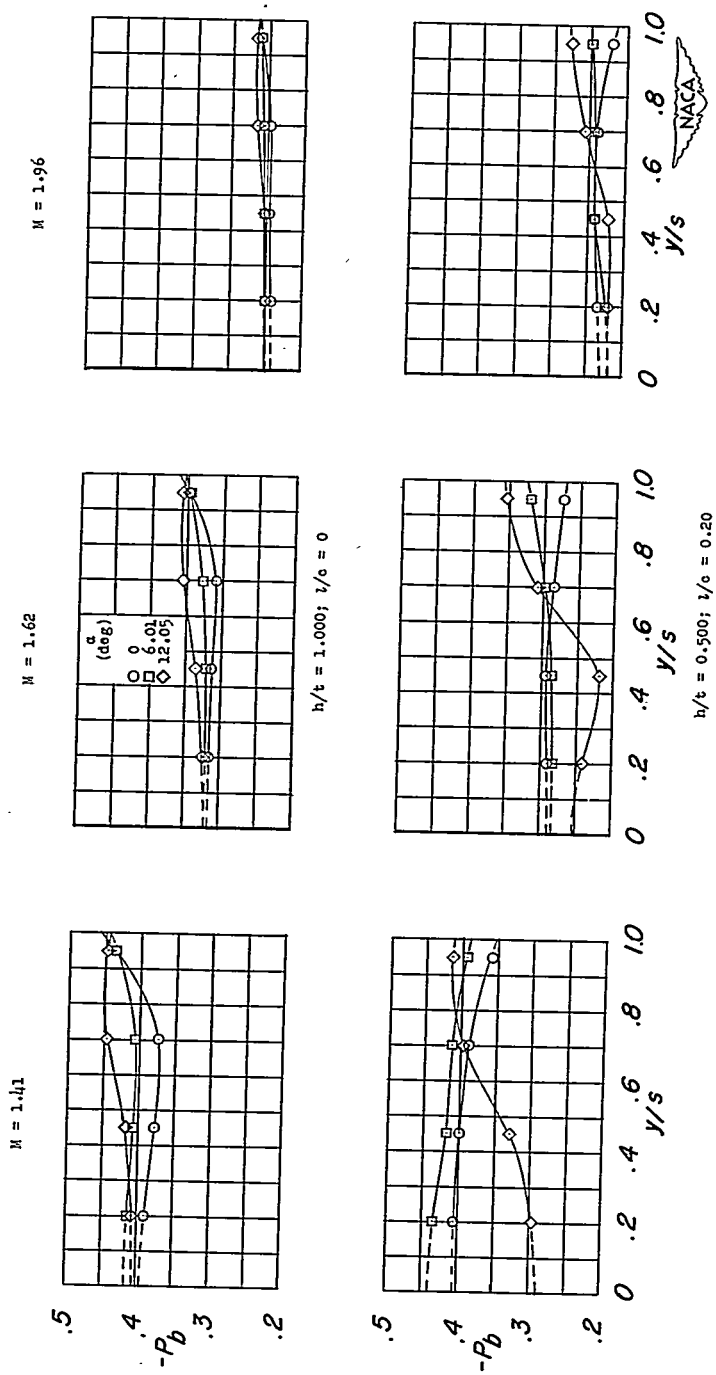

(b) A = 2.7; Λ = 0°; λ = 1.0; t/c = 0.060.

Figure 4.- Continued.

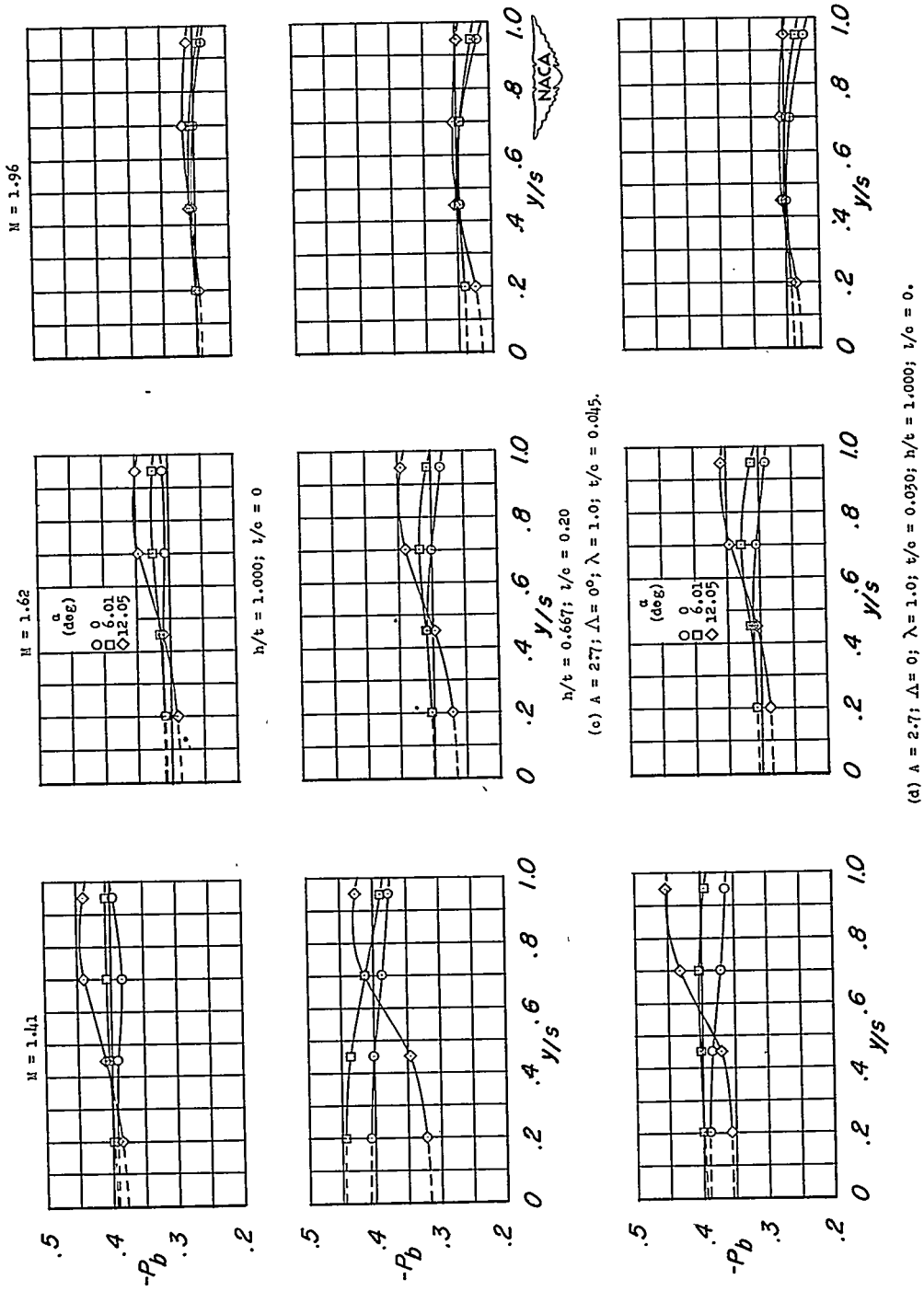

(c) A = 2.7; Λ = 0°; λ = 1.0; t/c = 0.045.

(d) A = 2.7; Λ = 0; λ = 1.0; t/c = 0.030; h/t = 1.000; t/c = 0.

Figure 4.- Continued.

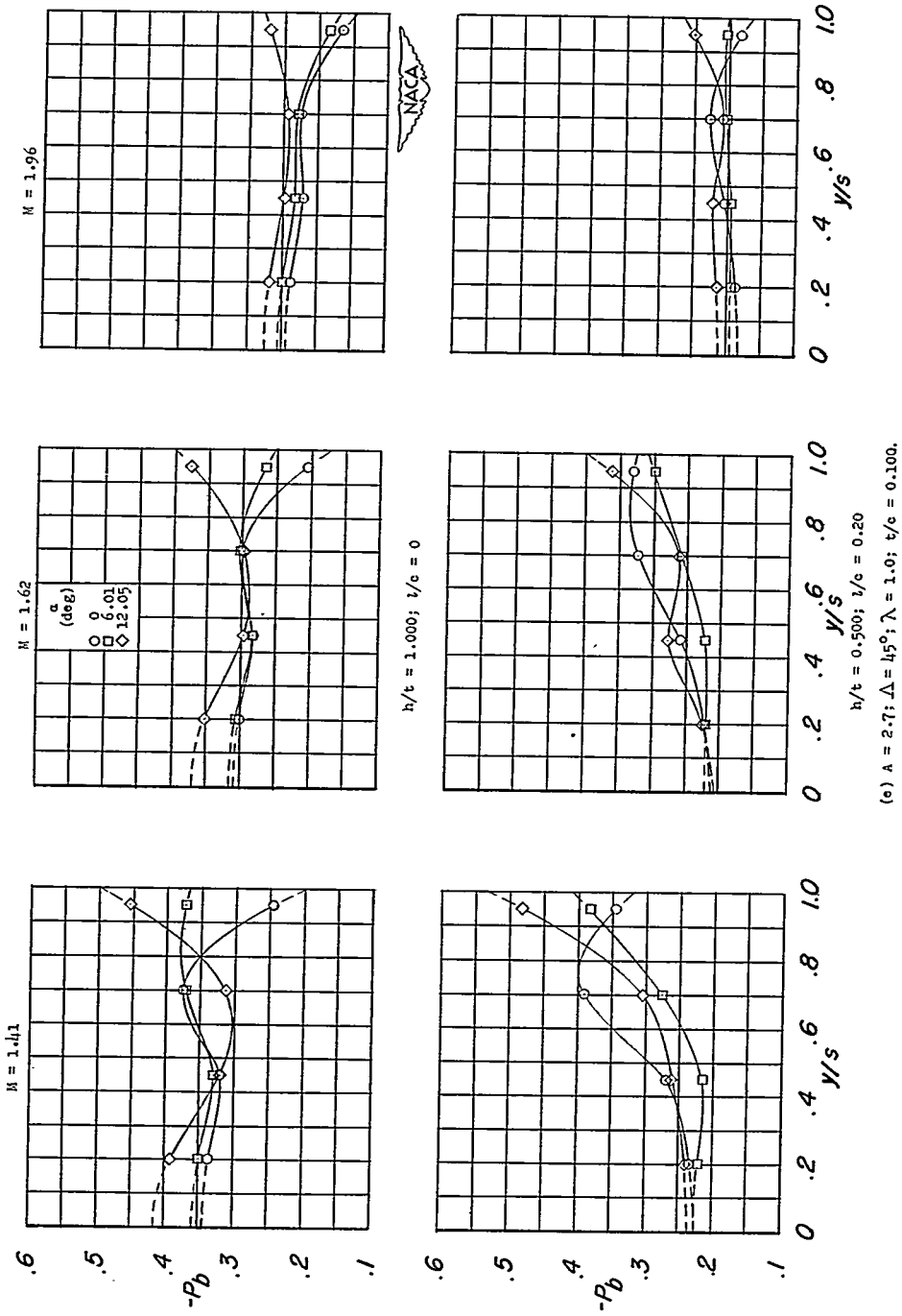

(c) A = 2.7; Λ = 45°; λ = 1.0; t/c = 0.100.

Figure 4.- Continued.

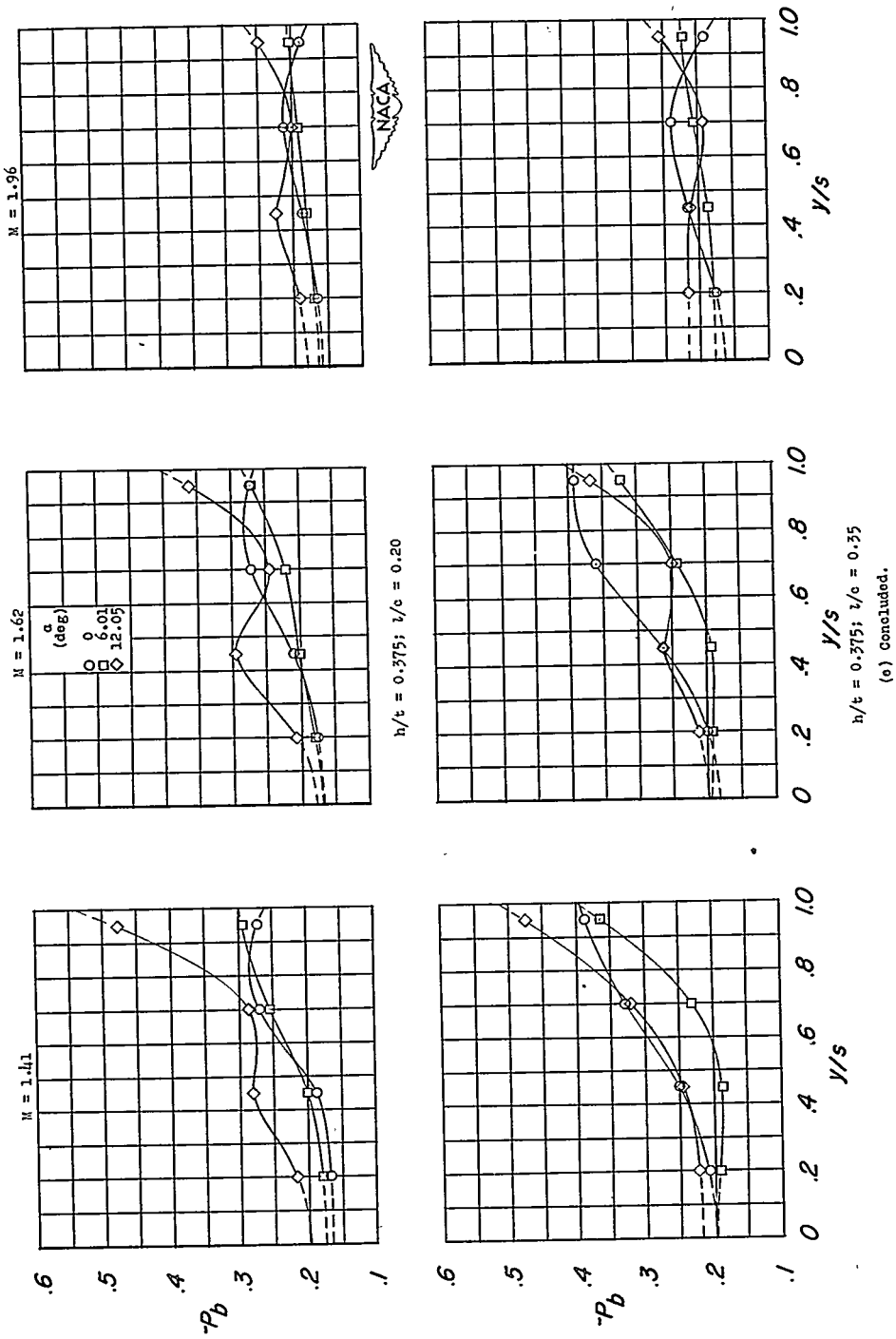

(e) Concluded.

Figure 4.- Continued.

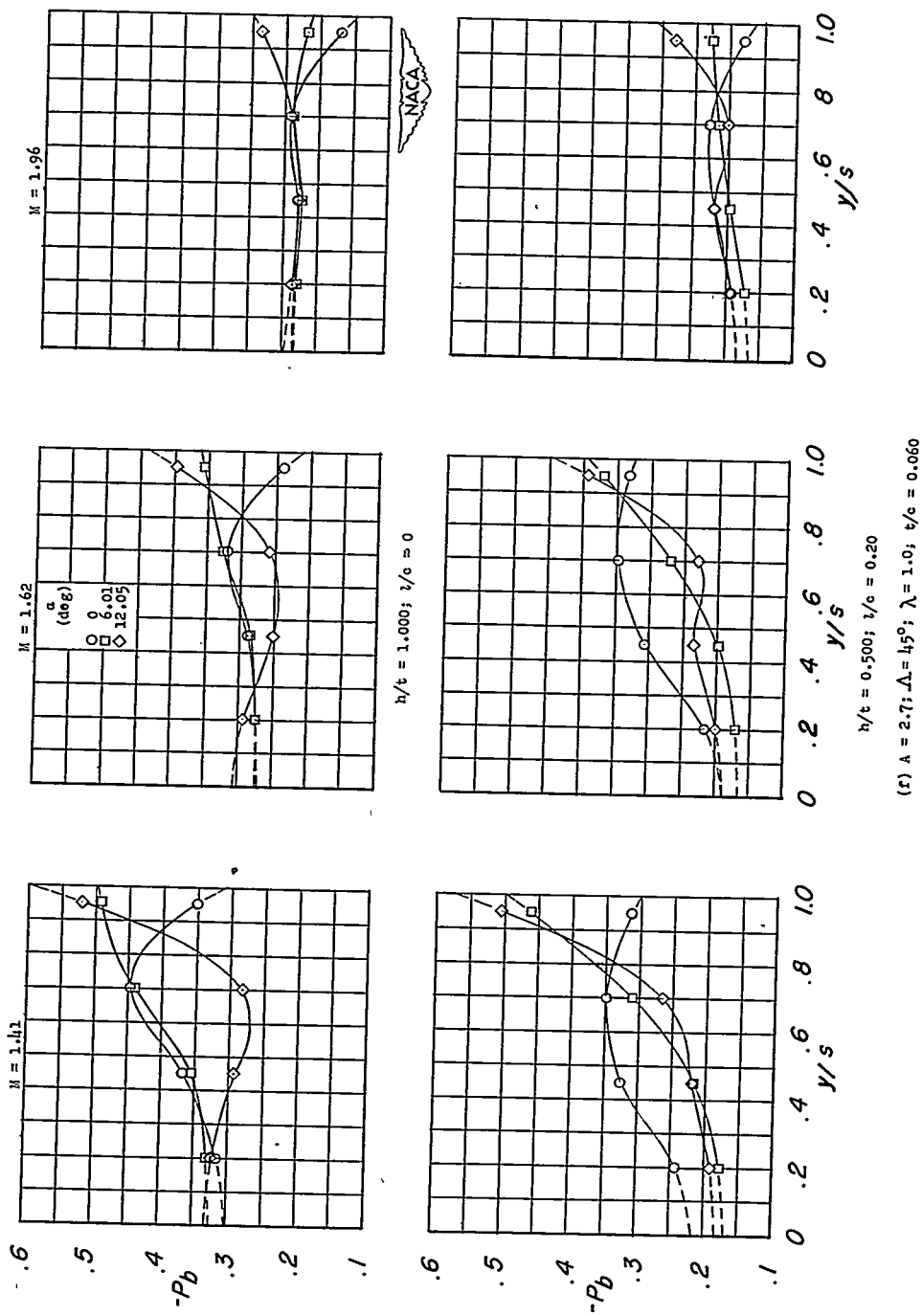

Figure 4.- Continued.

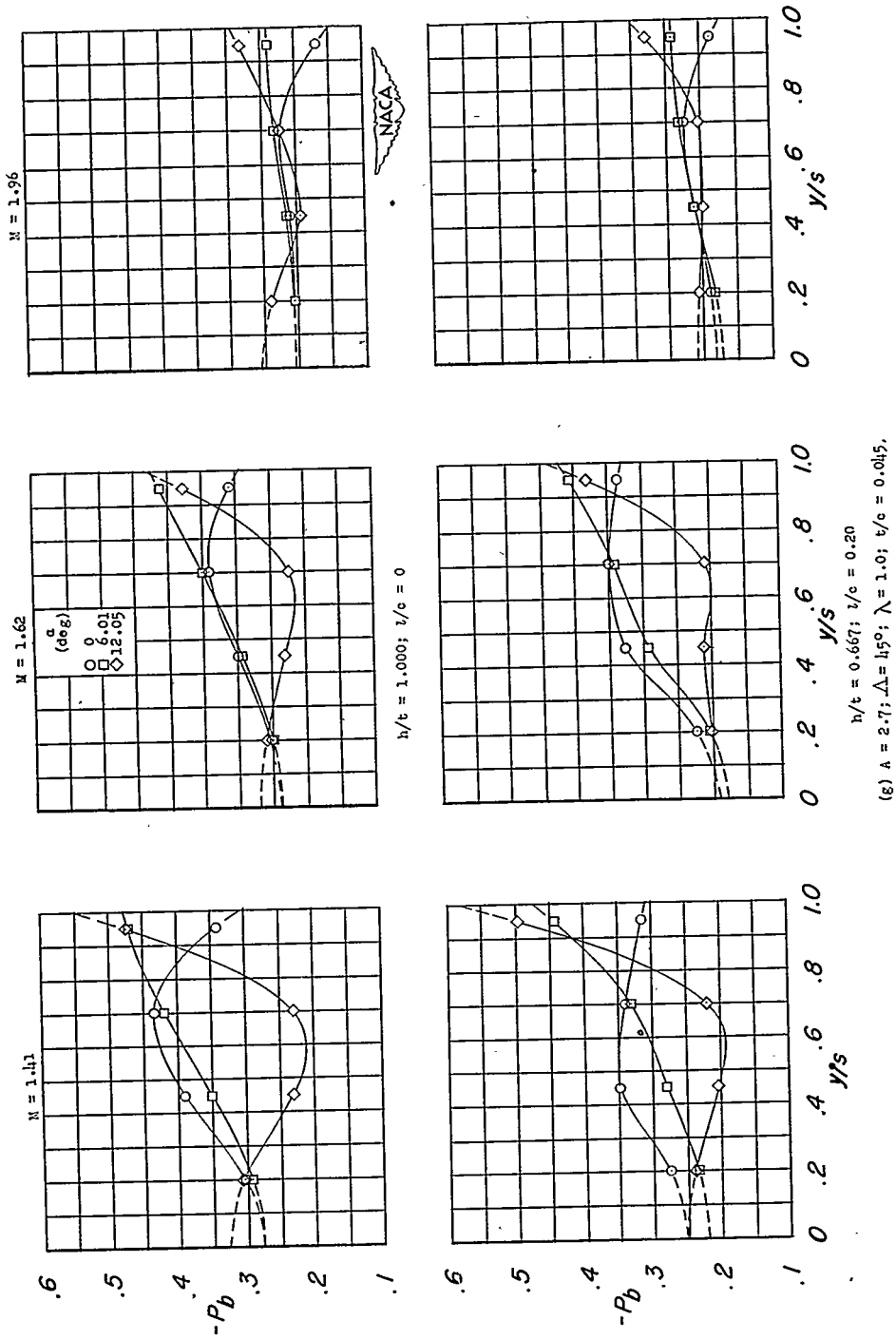

(g) A = 2.7; Λ = 45°; λ = 1.0; t/c = 0.045.

Figure 4.- Continued.

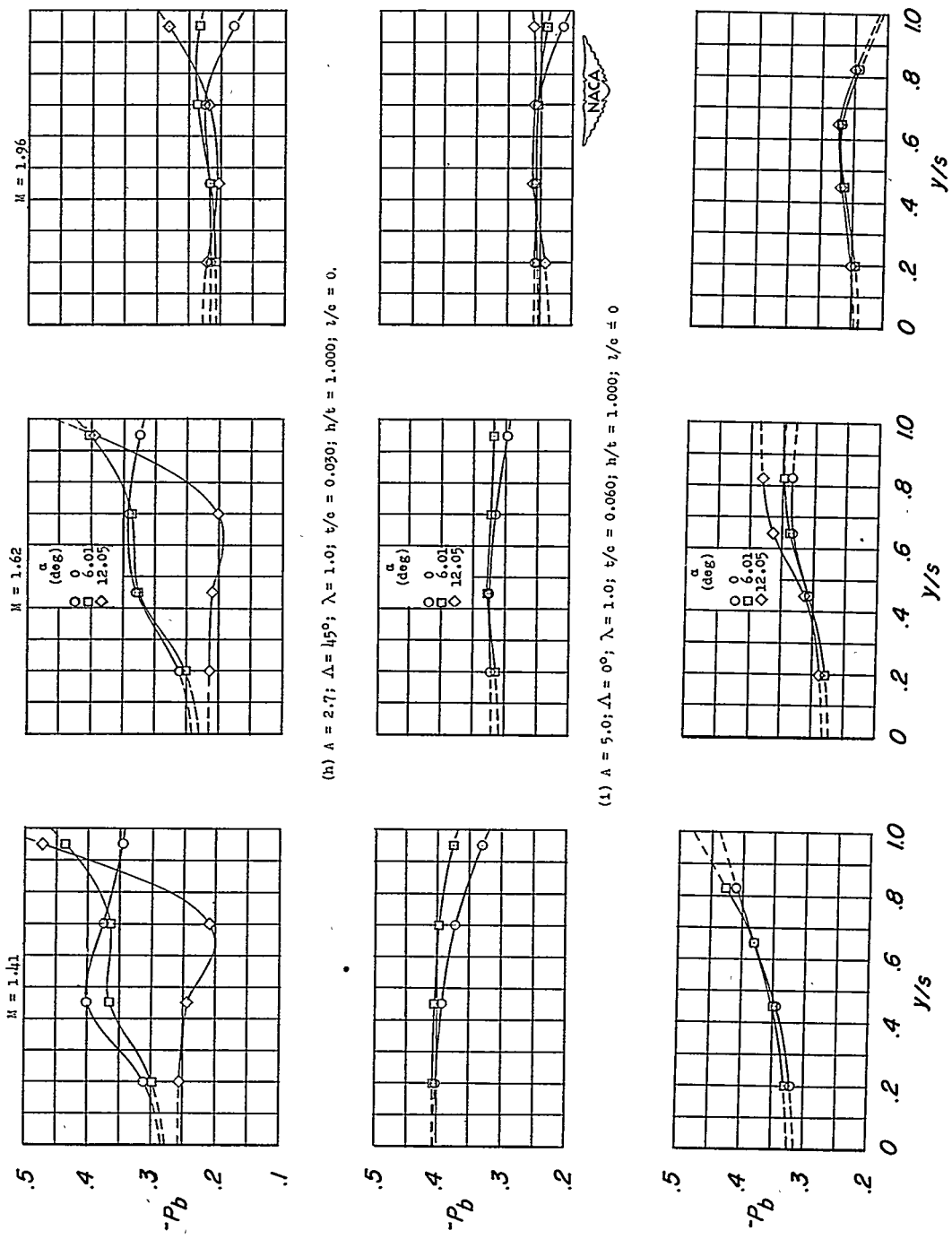

(h) A = 2.7; Δ = 45°; λ = 1.0; t/c = 0.030; h/t = 1.000; i/c = 0.

(i) A = 5.0; Δ = 0°; λ = 1.0; t/c = 0.060; h/t = 1.000; i/c = 0

(j) A = 4.0; Δ = 45°; λ = 0; t/c = 0.060; h/t = 1.000; i/c = 0.

Figure 4.- Concluded.

Type of boundary layer

T - Turbulent

ST - Separated turbulent or unusually thick turbulent

L - Laminar

TL - Thin laminar

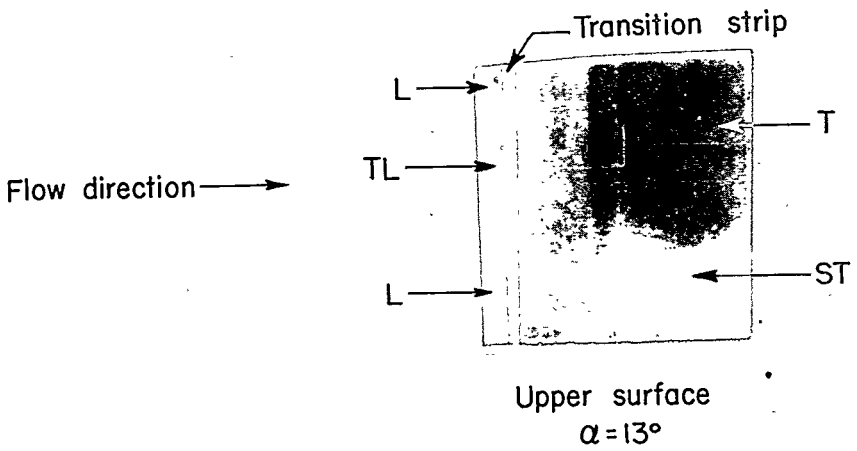

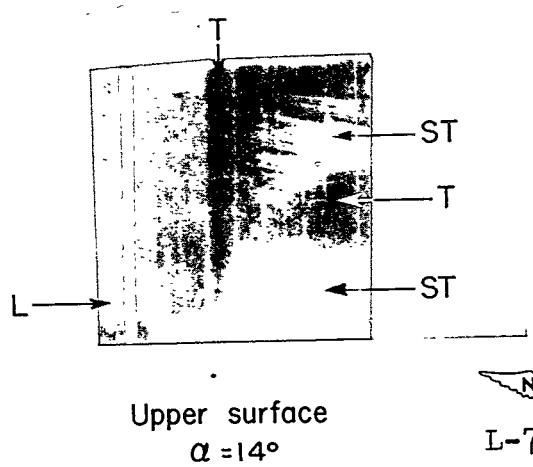

NACA

L-75091

Figure 5.- Liquid-film photographs at $M = 1.41$ of a rectangular wing. $\frac{t}{c} = 0.100$; $\frac{h}{t} = 0.375$; $\frac{l}{c} = 0.50$.

Type of boundary layer

T - Turbulent

ST - Separated turbulent or unusually thick turbulent

L - Laminar

TL - Thin laminar

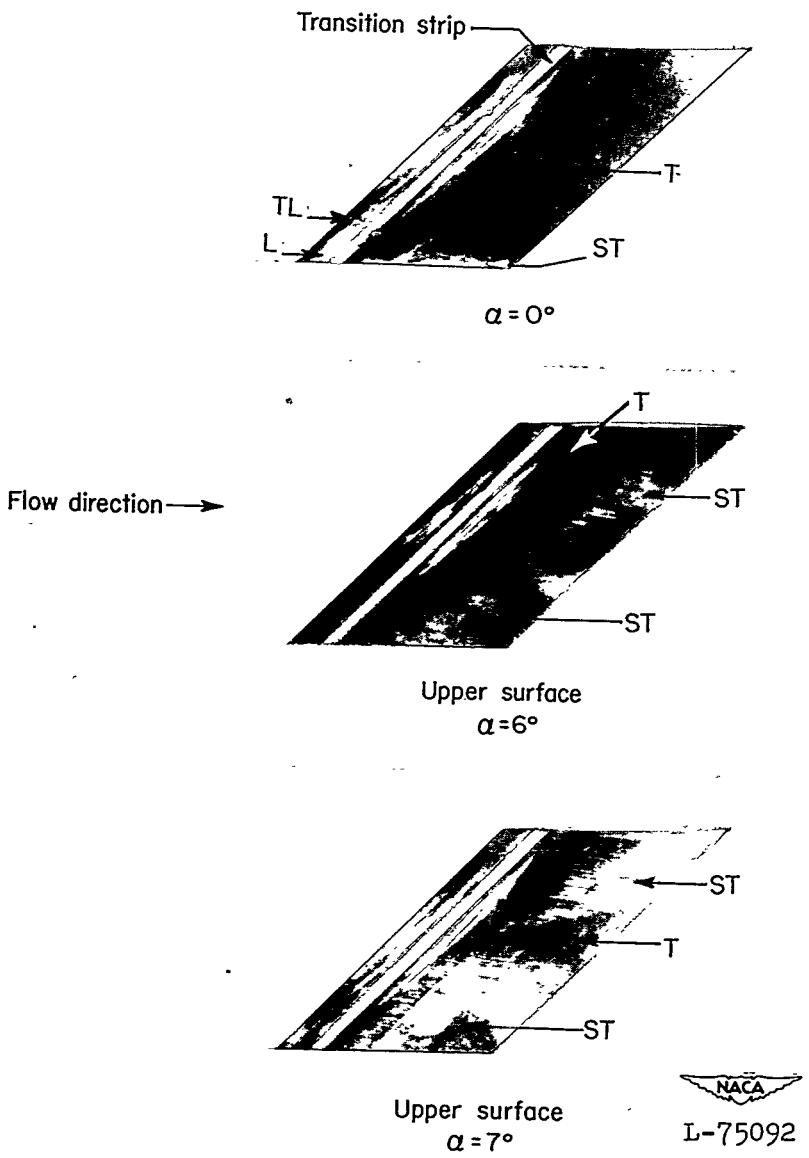

Figure 6.- Liquid-film photographs at $M = 1.41$ of a 45° swept wing. $\frac{t}{c} = 0.100$; $\frac{h}{t} = 0.375$; $\frac{l}{c} = 0.35$.

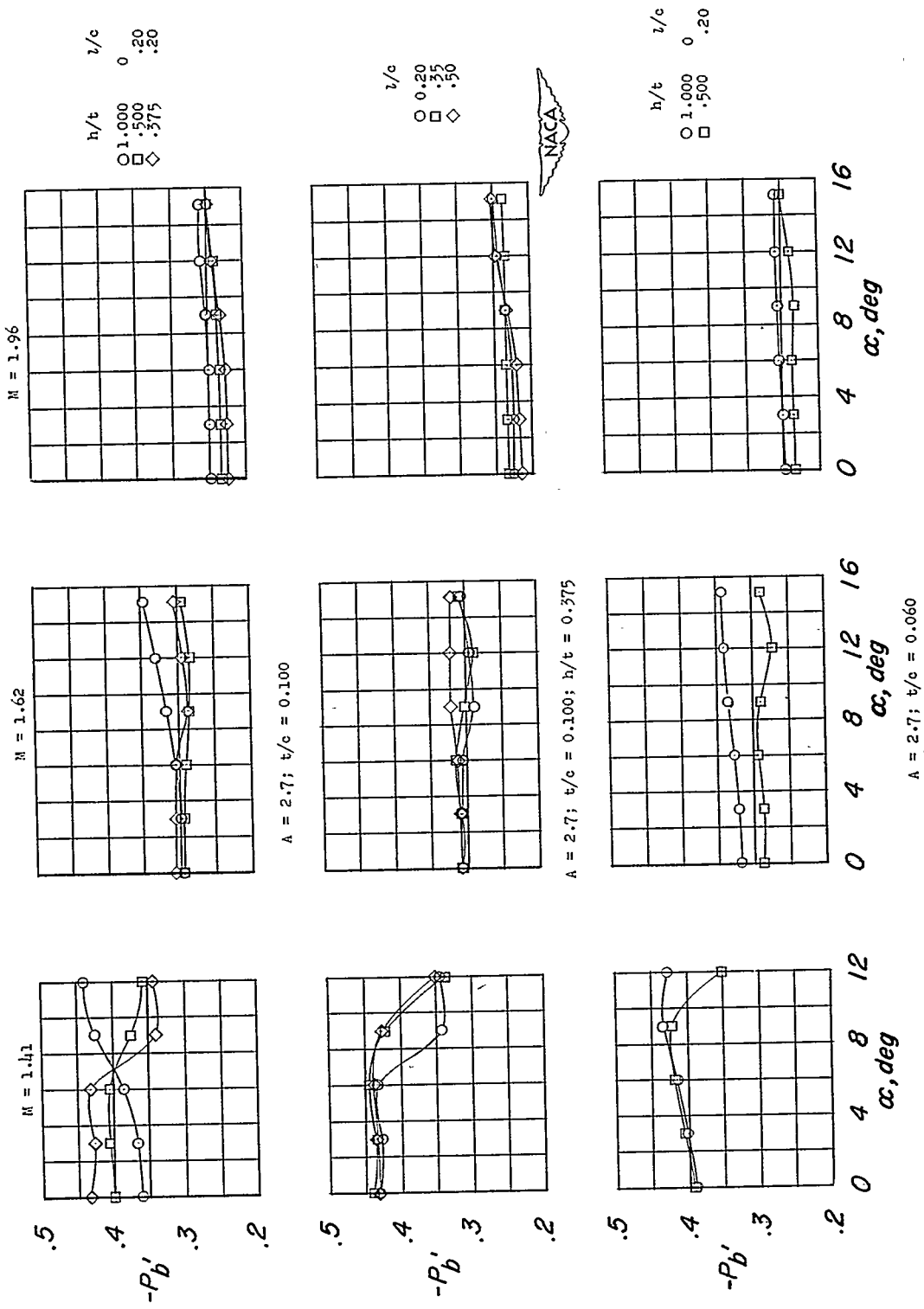

Figure 7.- Variations with angle of attack of average base pressure coefficients for rectangular wings.

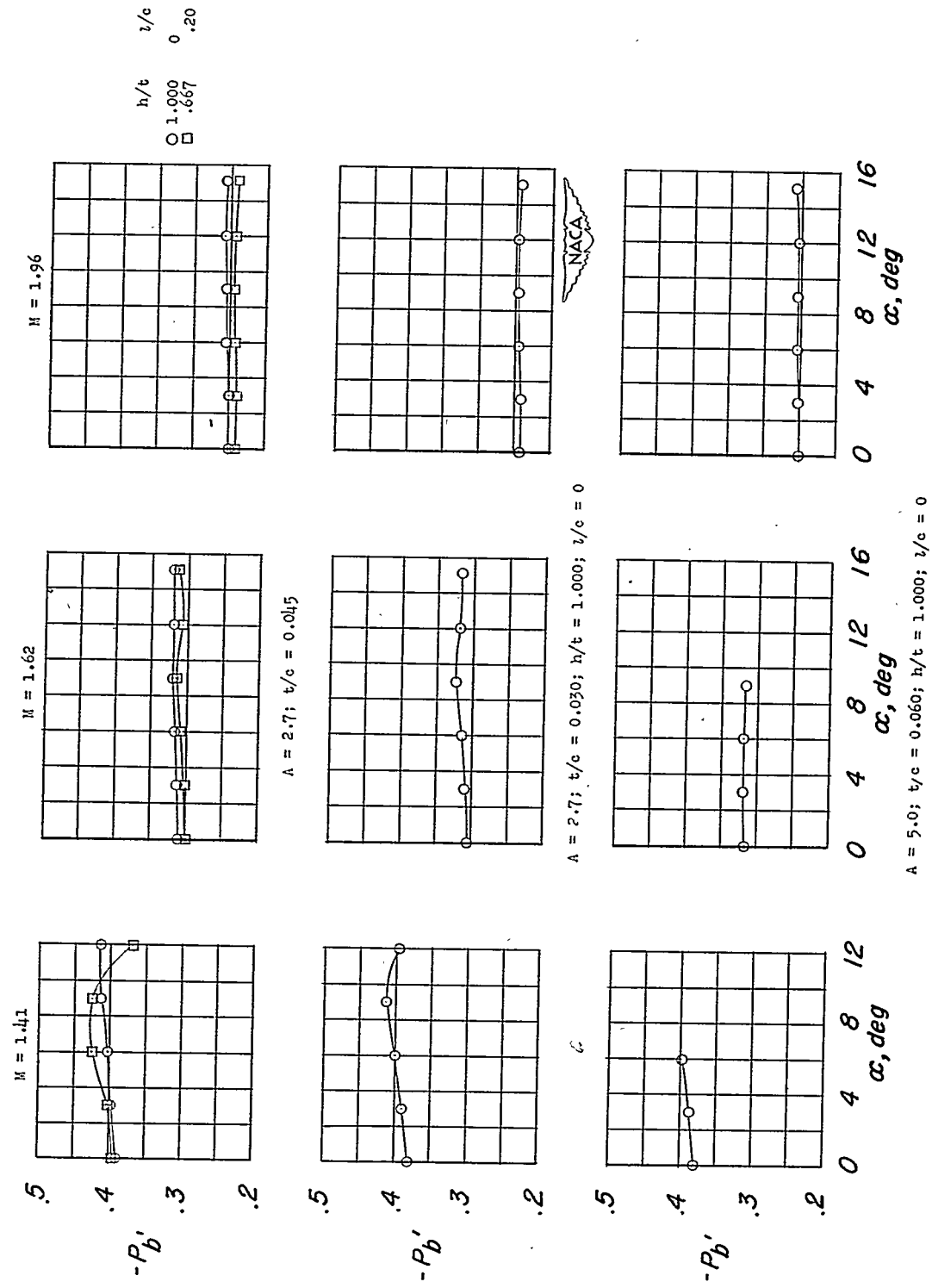

Figure 7.- Concluded.

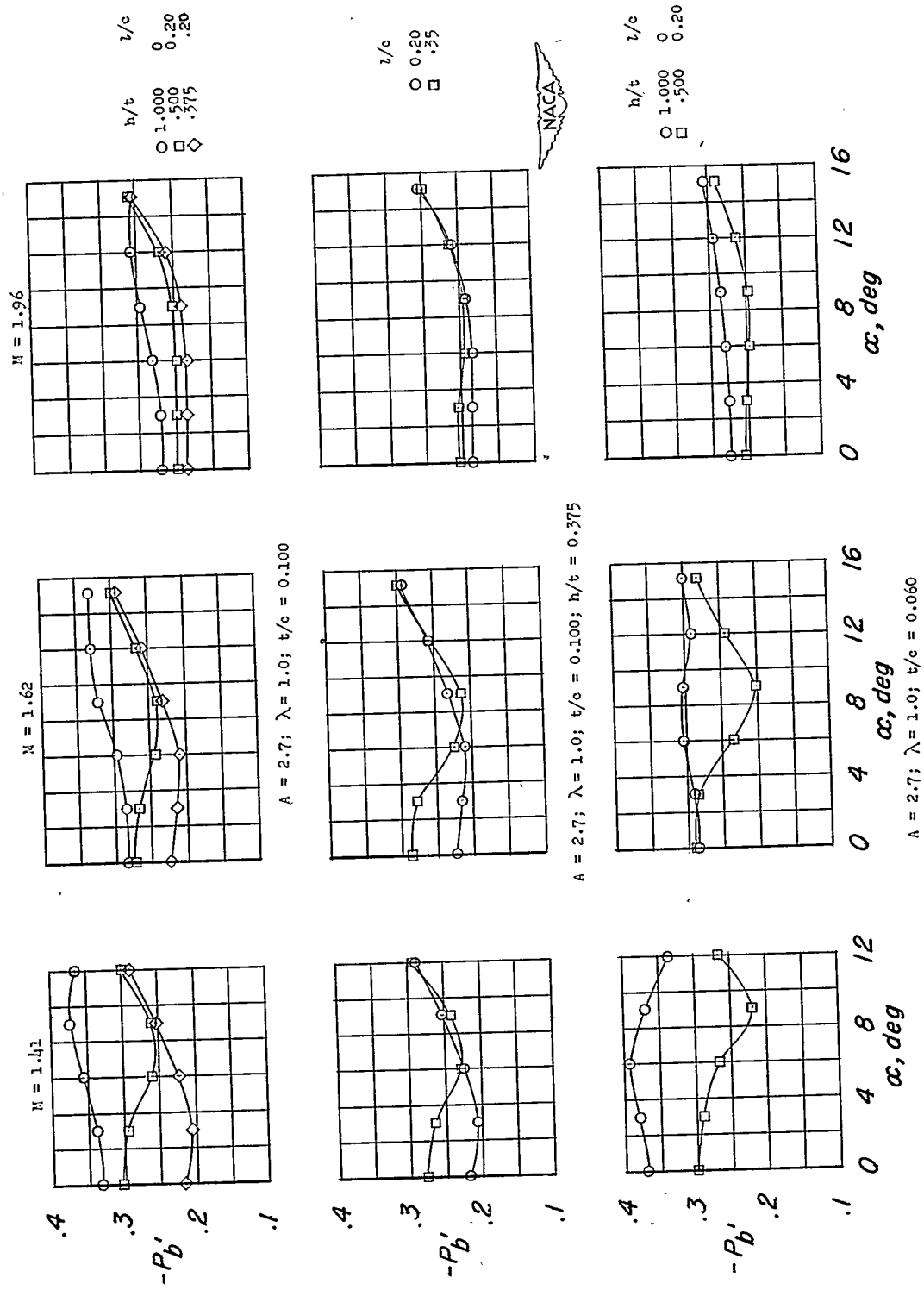

Figure 8.- Variations with angle of attack of average base pressure coefficients for 45° swept wings.

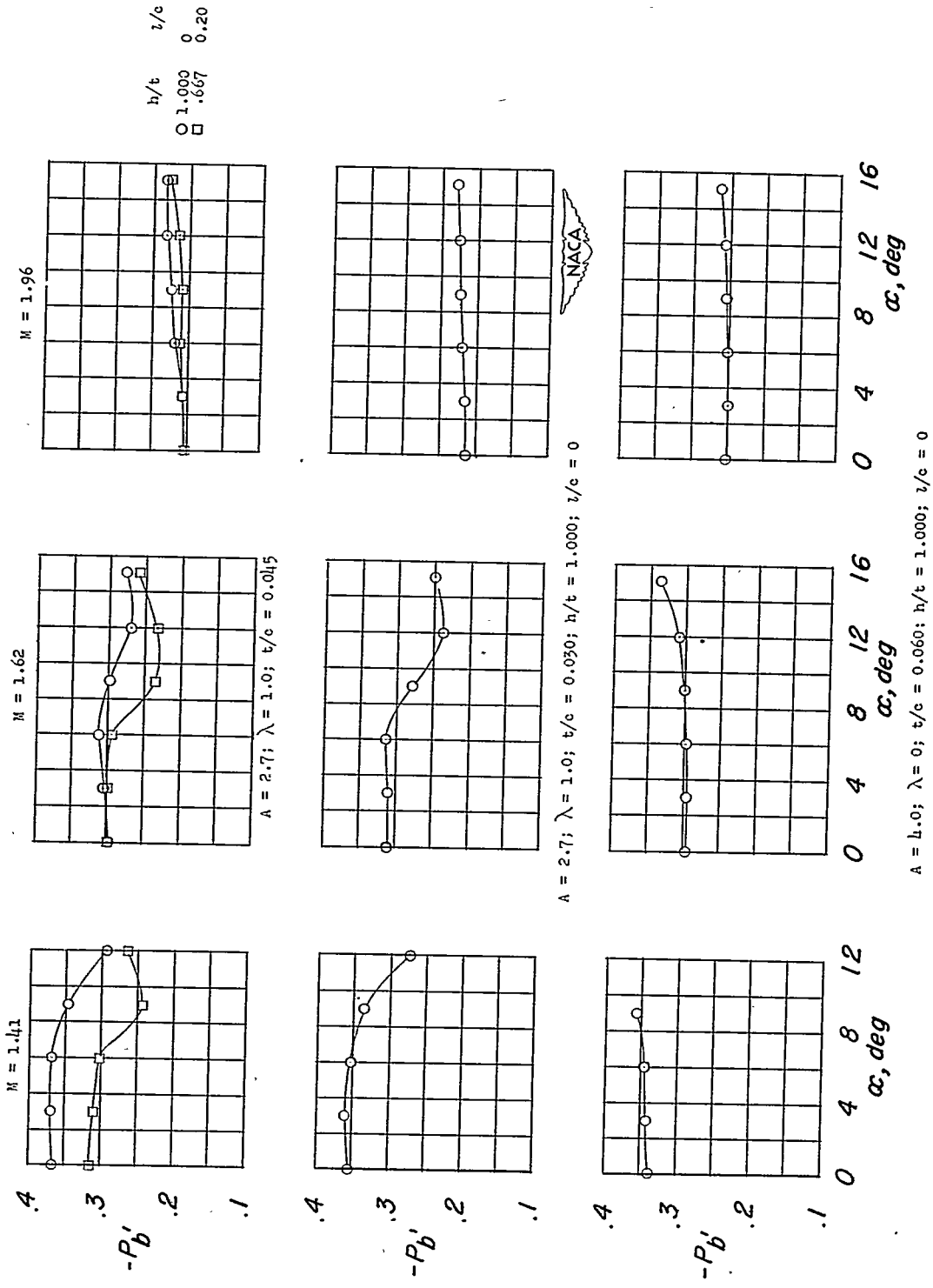

Figure 8.- Concluded.

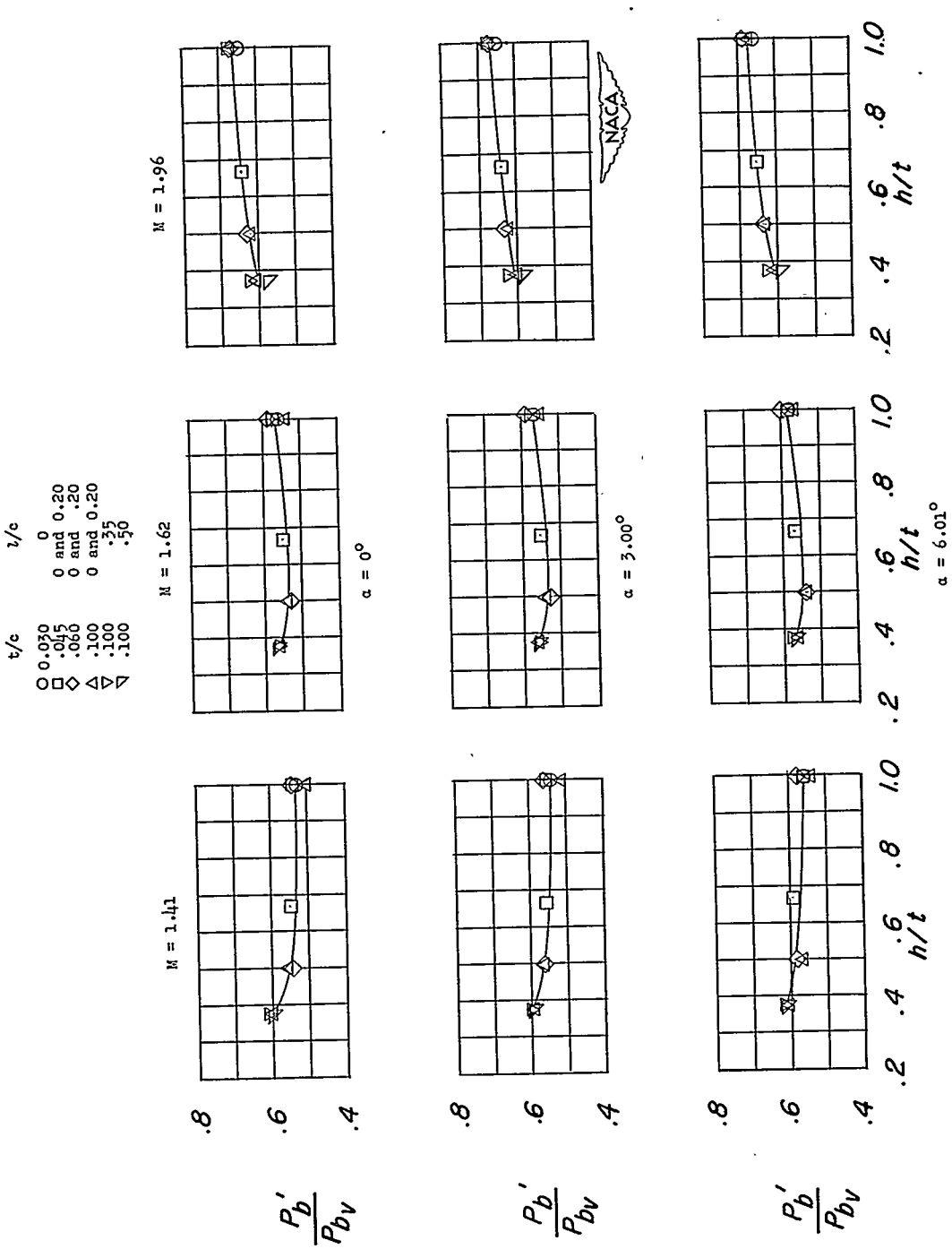

Figure 9.- Summary variations with wing section of average base pressure coefficients for unswept wings. A = 2.7; λ = 1.0.

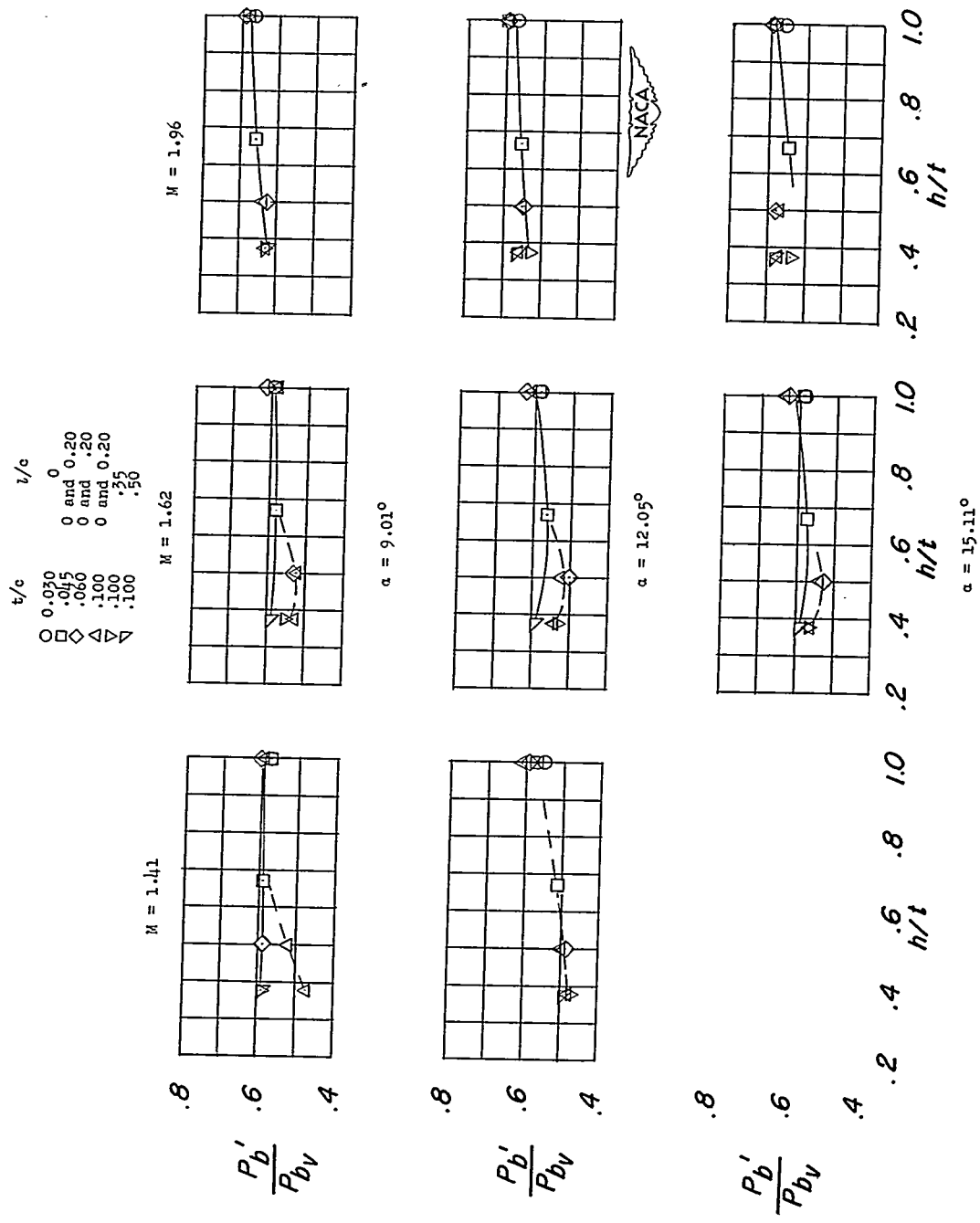

Figure 9.- Concluded.

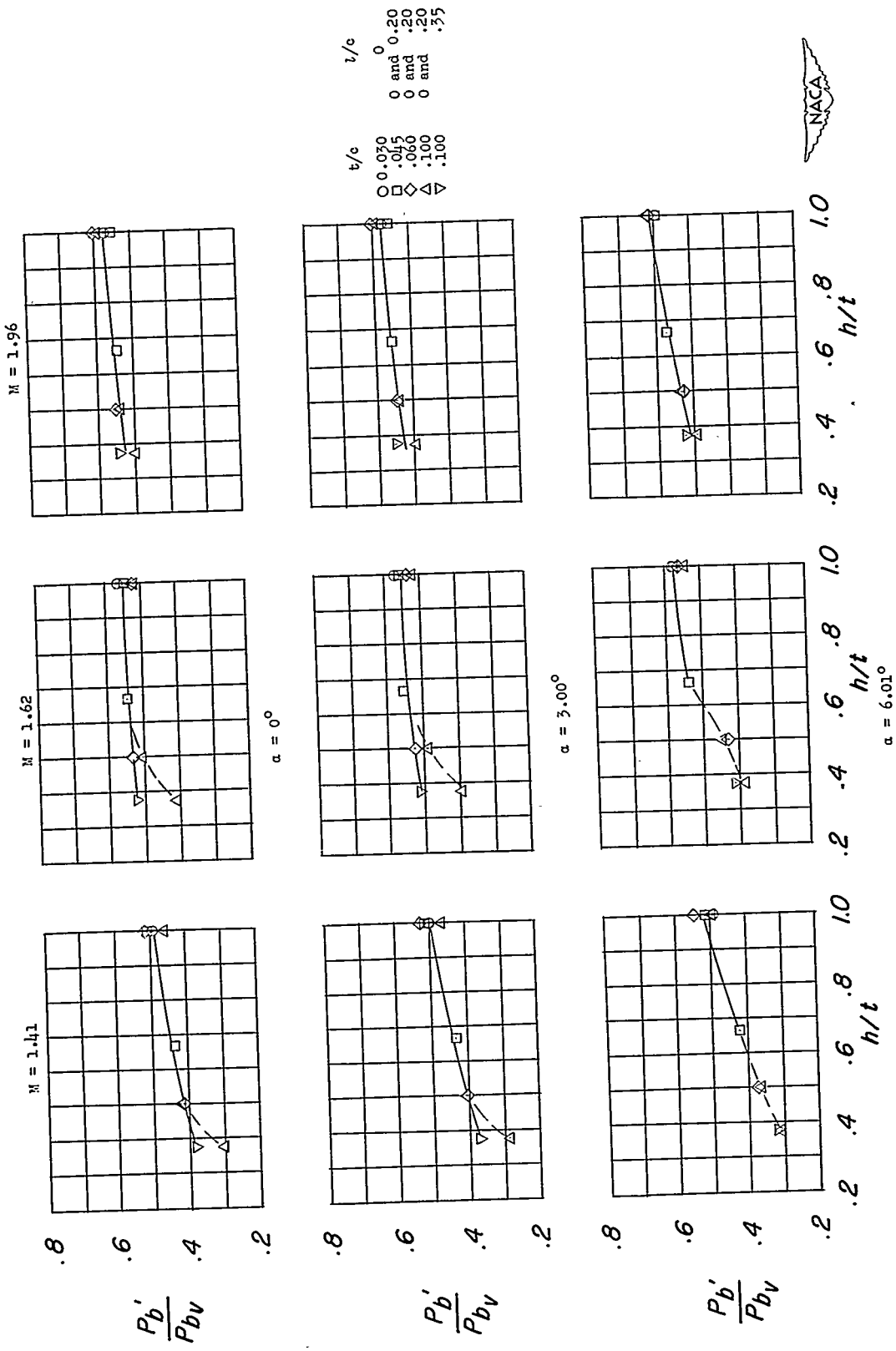

Figure 10.- Summary variations with wing section of average base pressure coefficients for 45° swept wings. A = 2.7; λ = 1.0.

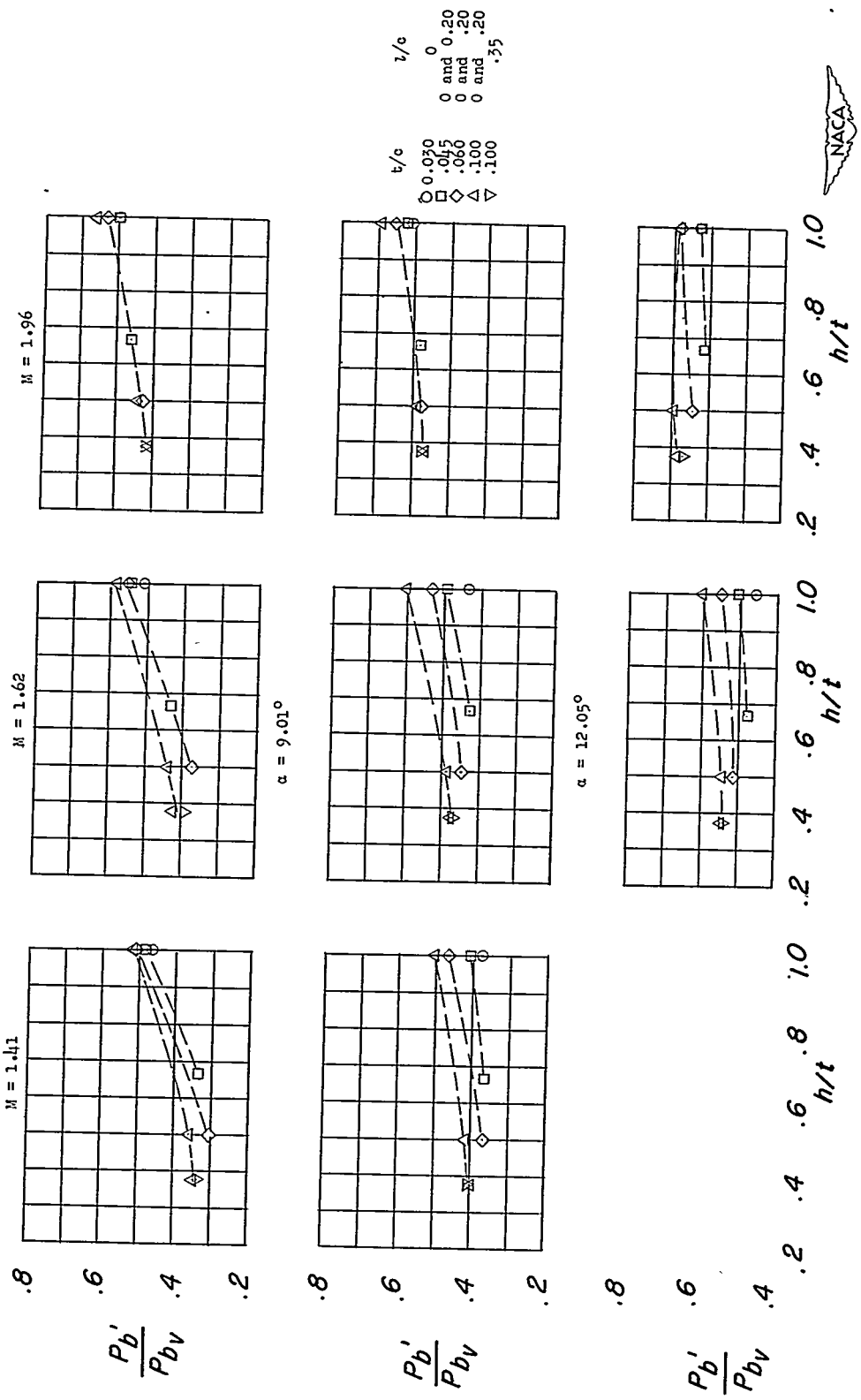

Figure 10.- Concluded.

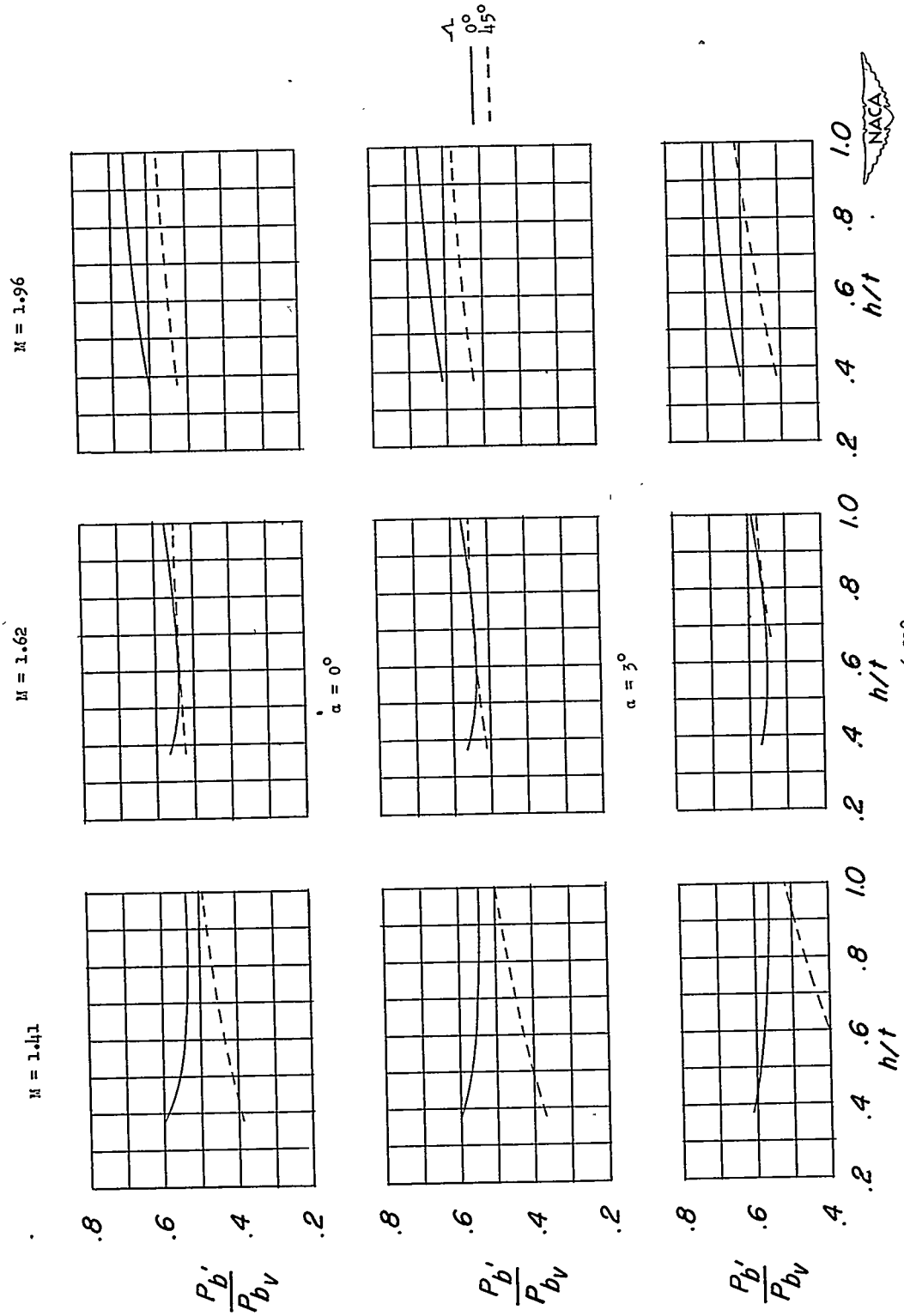

Figure 11.- Comparison of summary effects of section on base pressure of 0° and 45° swept wings of aspect ratio 2.7.

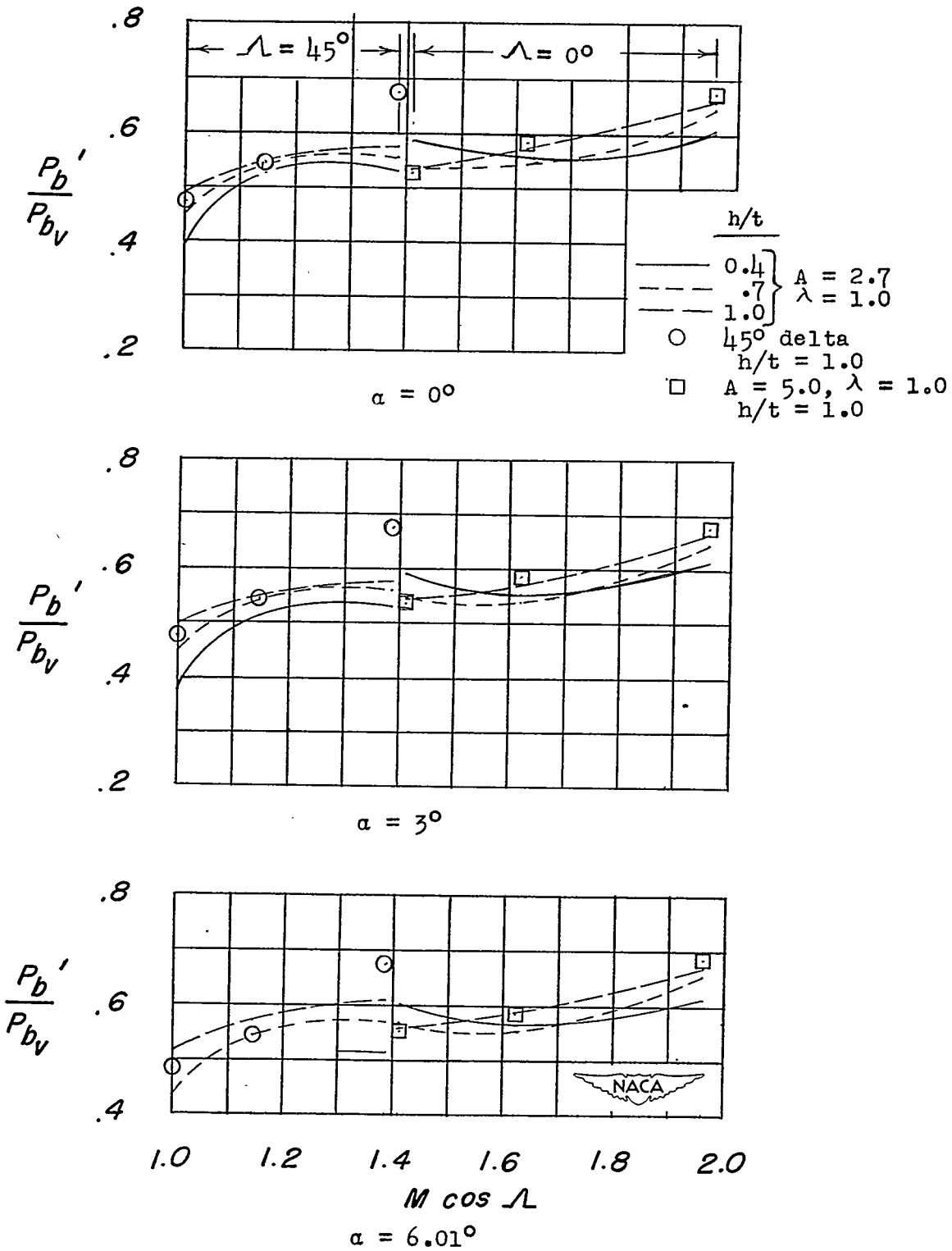

Figure 12.- Summary of average base pressure coefficients from the present investigation.

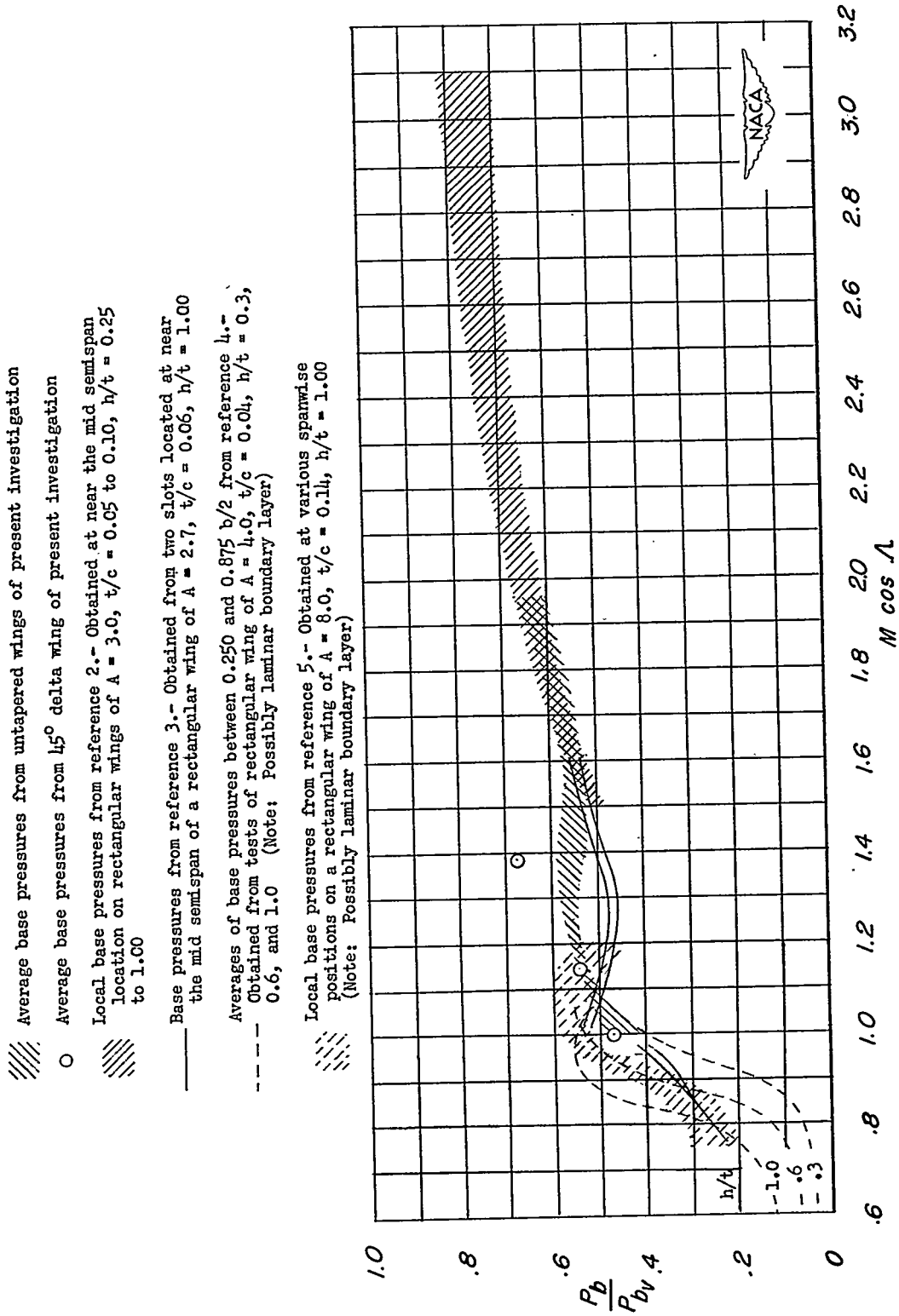

Figure 13.- Comparison of integrated base pressures from present investigation with base pressures from other facilities. $\alpha = 0^{\circ}$.

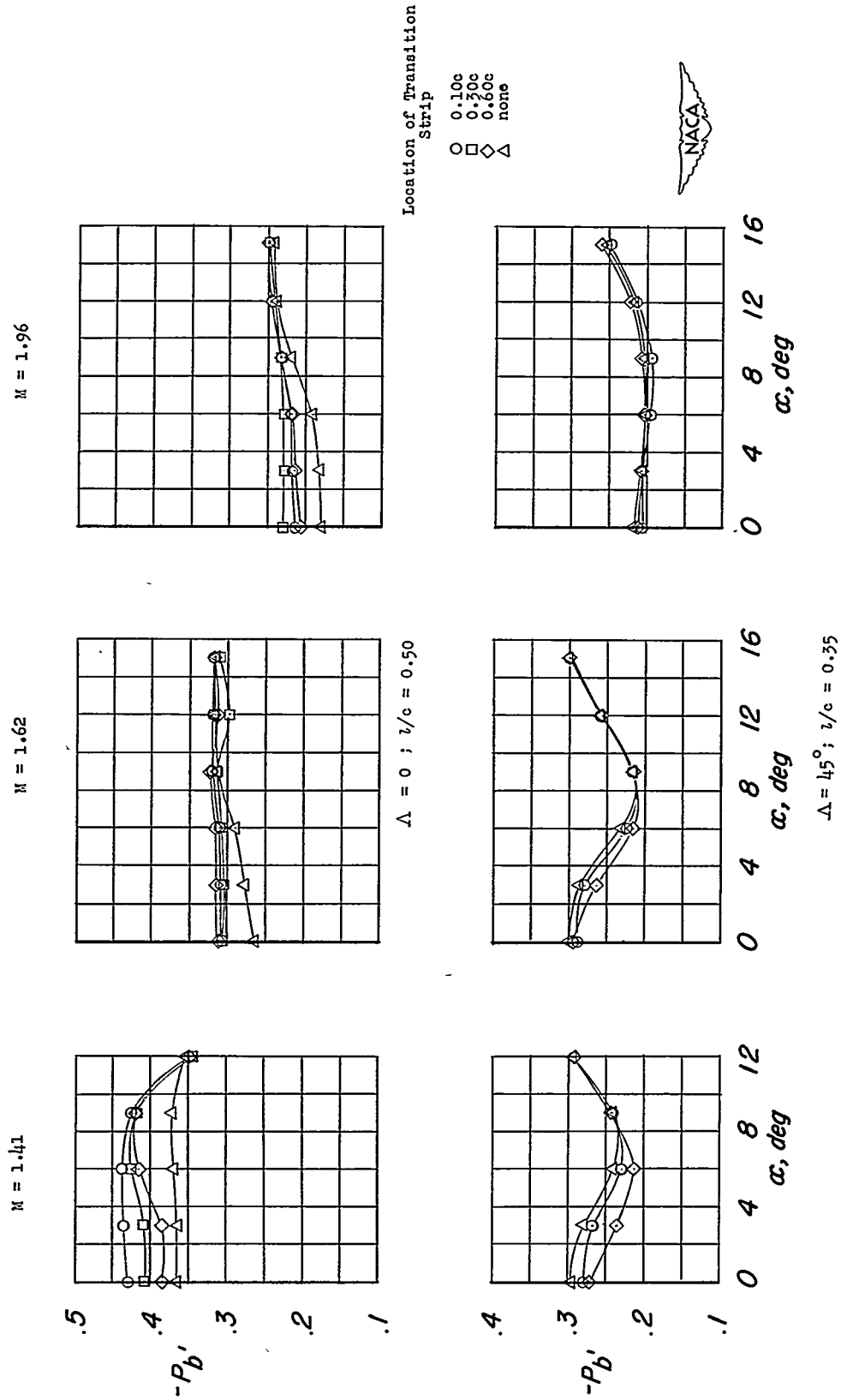

Figure 14.- Effects of various transition-strip locations on the average base pressures for untapered wings of aspect ratio 2.7 and 0° and 45° sweep. $\frac{t}{c} = 0.100$; $\frac{h}{t} = 0.375$.

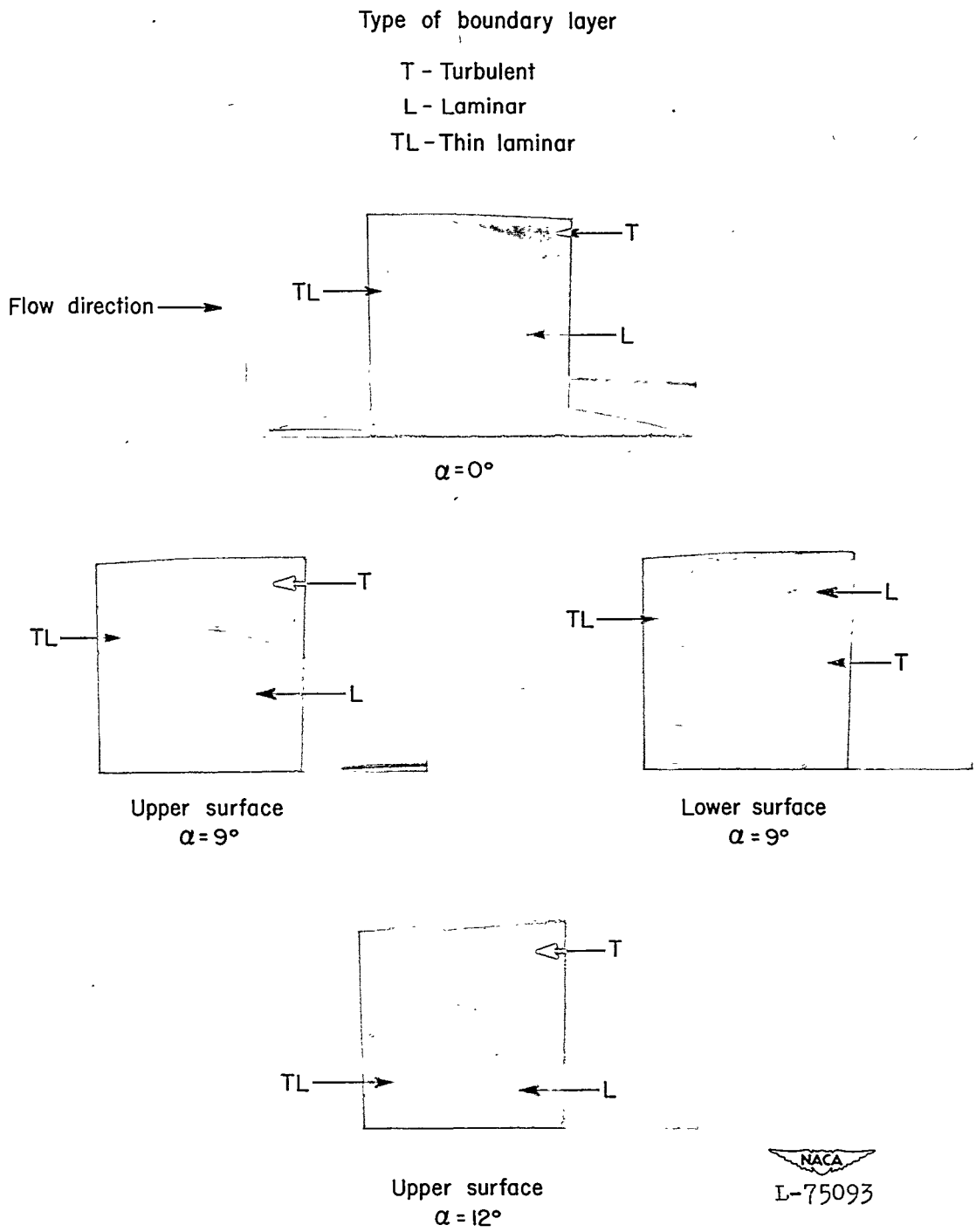

(a) M = 1.41.

Figure 15.- Liquid-film photographs of smooth rectangular wing. $\frac{t}{c} = 0.100$; $\frac{h}{t} = 0.375$; $\frac{l}{c} = 0.50$.

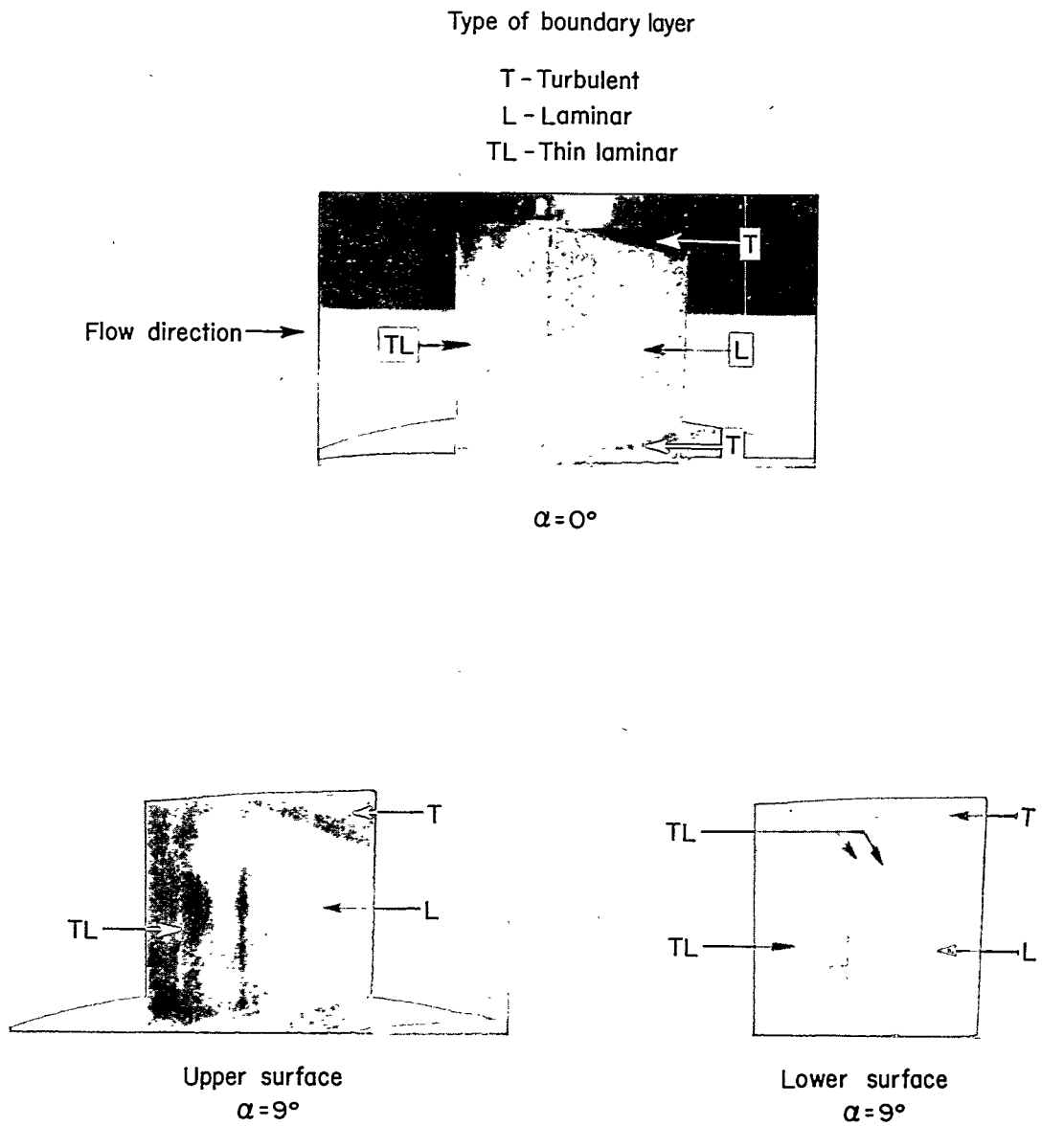

(b) M=1.96

Figure 15.- Concluded.

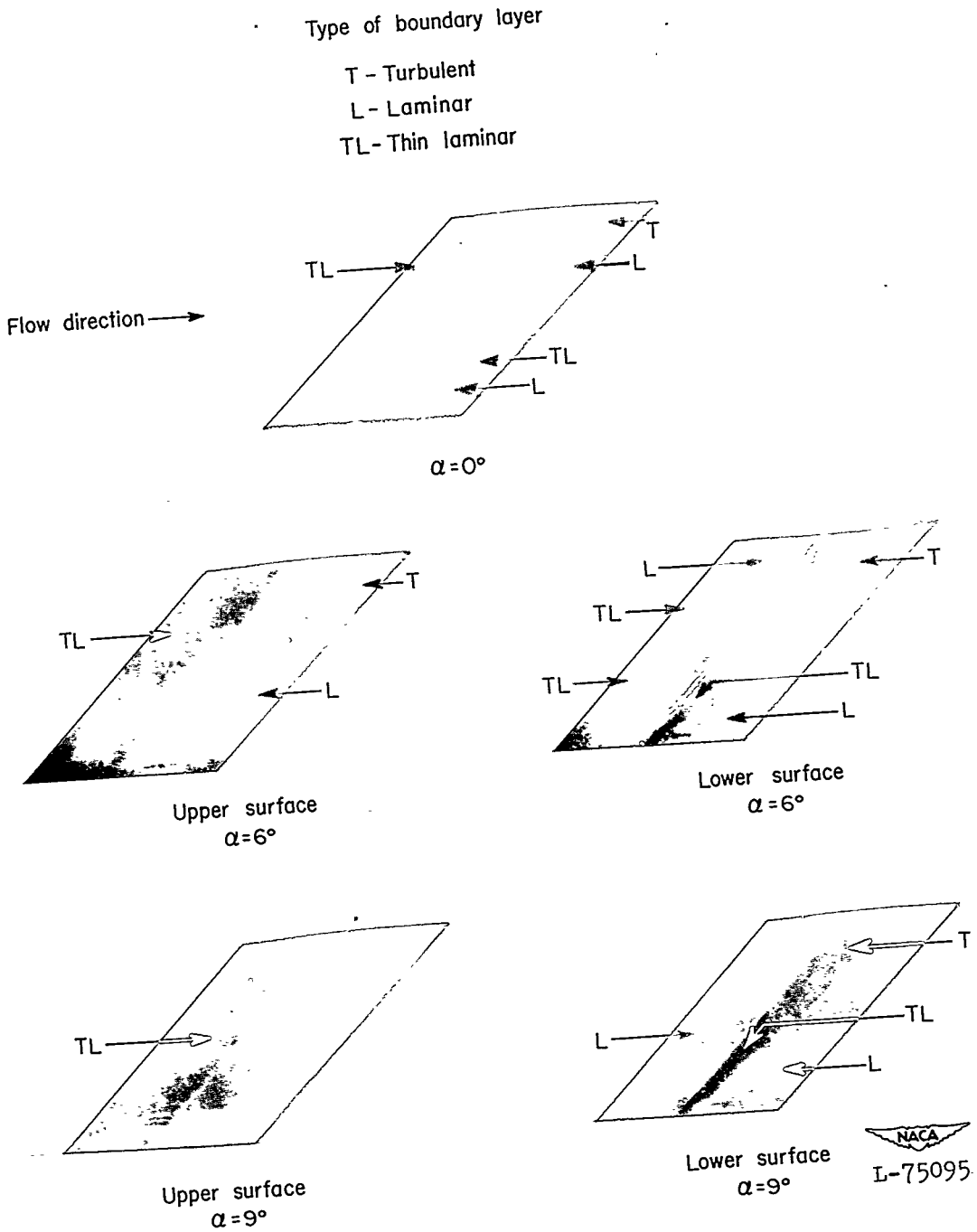

(a) M = 1.41.

Figure 16.- Liquid-film photographs of smooth 45° swept wing. $\frac{t}{c} = 0.100$; $\frac{h}{t} = 0.375$; $\frac{l}{c} = 0.35$.

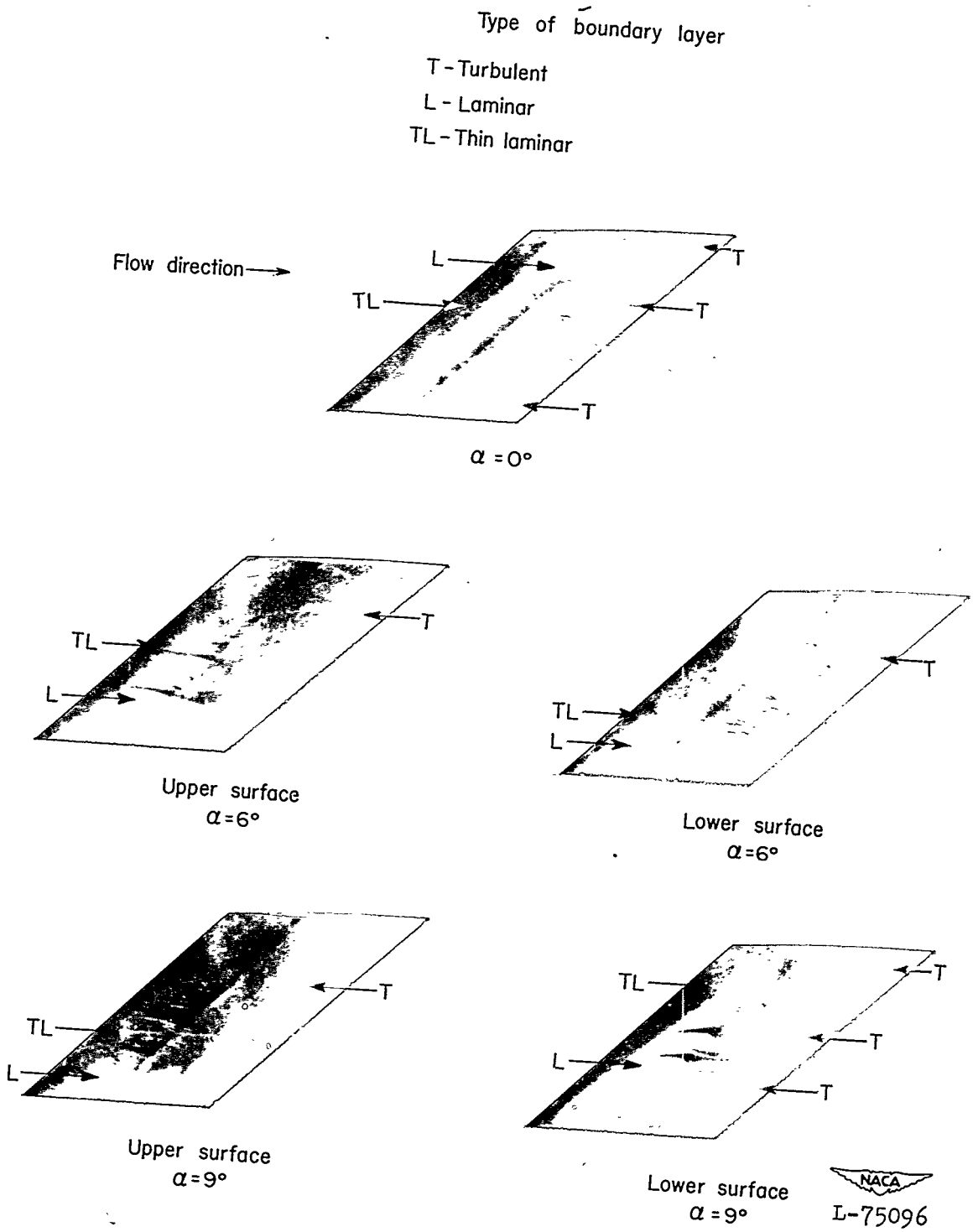

(b) M = 1.96.

Figure 16.- Concluded.